CDF/PHYS/ANA/CDF7040
Version 1.0
December 17, 2004

Search for Lepton-Photon events

Andrei Loginov
Institute for Theoretical and Experimental Physics,
Moscow, Russia
Henry Frisch
Enrico Fermi Institute, University of Chicago
Chicago, IL 60637

Abstract

We present a search for the anomalous production of events with a high E_T photon and a high E_T electron or muon using 200 pb^{-1} of data taken with the CDF detector in Run II at the Tevatron. The search includes measurements of the production of events with additional high E_T leptons, photons, missing transverse energy, or total transverse energy. The kinematic selection criteria search are the same as in the CDF Run I search that found a possible excess in the $\ell\gamma\not{E}_{\mathrm{T}}$ channel and several lepton-photon events with multiple photons and/or leptons. We find 14 $\ell\gamma\not{E}_{\mathrm{T}}$ events (8 in the $e\gamma$ channel and 6 in the $\mu\gamma$ channel) versus a Standard Model expectation of $18.81 \pm .95$ ($11.46 \pm .70$ and $7.37 \pm .64$) events. There are 13 (7 and 6) multilepton+gamma and 0 (0 and 0) multigamma+lepton events, versus expectations of $14.38 \pm .33$ ($9.46 \pm .27$ and $4.94 \pm .19$) and $.02040 \pm .0049043$ ($.01664 \pm .0045196$ and $.00480 \pm .0019040$) events, respectively.

Contents

1 Introduction **3**
1.1 The Gamma-Lepton Signature . . . 3
1.2 Run I Results and the Present Analysis. . . . 4

2 The CDF Detector **5**

3 Selection of Photon-Lepton Candidates **5**
3.1 Datasets . . . 5
3.2 Good Run Selection . . . 6
3.3 Luminosity . . . 6
3.4 Muon Identification . . . 6
3.4.1 Tight Central Muons . . . 6
3.4.2 Loose Central Muons . . . 9
3.4.3 Muon Control Sample . . . 9
3.5 Electron Identification . . . 13
3.5.1 Tight Central Electrons . . . 13
3.5.2 Loose Central Electrons . . . 14
3.5.3 Plug Electrons . . . 15
3.5.4 Electron Control Sample . . . 15
3.6 Photon Identification . . . 20
3.6.1 Photons in the Muon Subsample . . . 20
3.6.2 Photons in the Electron Subsample . . . 20
3.6.3 Photon Control Sample . . . 21
3.7 Missing E_T Identification . . . 21
3.8 Criteria for Additional Objects In the Event . . . 24

4 Standard Model Predictions **24**
4.1 Introduction: The Matrix Element Generators . . . 24
4.2 Checks . . . 24
4.2.1 Comparison of different samples at GENERATOR and HEPG levels . . . 24
4.2.2 Lepton E_T and P_T Resolution: Comparison of HEPG and Reconstructed Values . . . 29
4.3 The SM Diboson Processes $W\gamma$ and $Z^0\gamma$ as Sources of Lepton-Photon Events . . . 30
4.3.1 Expected rates from $W\gamma$ . . . 30
4.3.2 Expected Rates from $Z^0\gamma$ . . . 32
4.4 The SM $W\gamma\gamma$, $Z^0\gamma\gamma$ Processes as Sources of Lepton-Photon Events . . . 33
4.4.1 $W\gamma\gamma$ . . . 34
4.4.2 $Z^0\gamma\gamma$ . . . 35
4.5 Summary of $W\gamma$, $Z^0\gamma$, $W\gamma\gamma$, $Z^0\gamma\gamma$ predictions . . . 36
4.6 Fakes . . . 36
4.6.1 Jet Faking Photon . . . 36
4.6.2 Electron Faking Photon . . . 36

5 Photon-Lepton Events **38**

6 Conclusions **39**

7 Acknowledgements **47**

8 Appendices **48**
8.1 Appendix A: List of good runs 48
8.2 Appendix B: List Of Lepton-Photon Events 48
8.2.1 Electron-Photon Events 48
8.2.2 Muon-Photon Events 53

1 Introduction

The Standard Model is an effective field theory that has so far described the fundamental interactions of elementary particles [1, 2, 3] remarkably well. However the model breaks down at energies of a few TeV, in that the cross-section for scattering of longitudinal W bosons would otherwise violate unitarity. The Fermilab Tevatron has the highest center-of-mass energy collisions of any present accelerator, with $\sqrt{s} = 1.96$ TeV, and thus has the potential to discover new physics. The production of two vector gauge bosons, precisely predicted in the Standard Model, provides a set of signatures in which to search for the production of new particles which couple to the SM gauge sector (the top quark being the last new example).

1.1 The Gamma-Lepton Signature

Why do we consider the gamma-lepton topology a good signature for observing new physics?

- The photon is coupled to electric charge, and thus is radiated by all charged particles, including the incoming states (important for searching for invisible final states);
- The photon is massless and thus kinematically easier to produce than the W or Z;
- The photon is stable which implies a high acceptance, as there are no branching ratios to ‘pay’;
- In searching for new particles/quantum numbers, the signature of *pairs* of gauge bosons

$$WW, WZ, ZZ, W\gamma, Z\gamma, \gamma\gamma$$

  is natural if pairs of particles with a conserved quantum number are produced because of flavor conservation in QCD.
- The production of a high-E_t photon and a high-P_t lepton is rare in the Standard Model, and so the backgrounds are low for searches.

The signature of high-E_t leptons and photons appears in a variety of New Physics scenarios. Supersymmetry, with its panoply of parameters and its heavy partners for the gauge bosons, one or more of which will have a photino component, easily provides models which produce final states with leptons and photons. For example, an initial model invoked low-energy supersymmetry with a neutralino LSP as a possible interpretation of the CDF $ee\gamma\gamma\not{E}_T$ event [4] via the process:

$$p\overline{p} \to \tilde{e}^+\tilde{e}^-(+X)$$
$$\tilde{e} \to \tilde{N}_2 + e$$
$$\tilde{N}_2 \to \tilde{N}_1\gamma,$$

where $\tilde{e}$ is the selectron (the bosonic partner of the electron), and $\tilde{N}_1$ and $\tilde{N}_2$ are the lightest and next-to-lightest neutralinos, the fermionic partners of the neutral bosonic states formed by mixing the fermionic partners W^0, the B, and the neutral Higgses into mass eigenstates.

Gauge-mediated models in which a photino decays into a gravitino, are also popular choices[5], and have the appealing feature that they have a natural dark matter candidate.

Further expanding the space of parameters, a more recent SUSY interpretation of the CDF $\mu\gamma\not{E}_{\mathrm{T}}$ events [6] is resonant smuon $\tilde{\mu}$ production with a single dominant R-parity violating coupling(Figure 1).

However the parameter space of SUSY models is so large, and there are so many other models beyond SUSY, including ones that have not yet been thought of, that we have adopted the strategy of testing the Standard Model predictions in promising signatures, and will set aside theoretical considerations until we have at least several times more data than the Run I samples. This strategy, known as 'Signature-based searches', is nothing more than testing the Standard Model [1], [2], [3], [7]. The current interest in models of extra dimensions [8], which can produce events with signatures of interest to this search, is a good example of an innovation that was searched for before it was thought of.

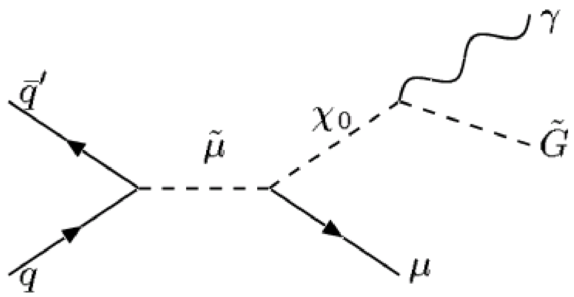

Figure 1: Resonant smuon production and subsequent decay, producing the $\mu\gamma\not{E}_{\mathrm{T}}$ signature

In summary, the strategy is to pick the channel

$$\text{photon} + \text{lepton} + \text{X}$$

where X can be any particle(s), with both the photon and the lepton to have large transverse momentum, in which to test the SM. The search includes looking for photon-lepton events with additional high E_T leptons, photons, missing transverse energy, or total transverse energy. The search complements SM measurements of $W\gamma$ and $Z\gamma$ production [9].

1.2 Run I Results and the Present Analysis.

The Run I results on the gamma+lepton+X production were intriguing [10, 11]. Two rare $\ell\ell\gamma\gamma+X$ events sparked signature-based searches in the $\gamma\gamma + X$ and $\ell\gamma + X$ channels. In addition, the measured event rate for the signature ℓ+γ+$\not{E}_{\mathrm{T}}$ was 2.8 sigma above the Standard Model predictions.

The Run I search was initiated by an anomaly in the data itself, and as such the 2.8 sigma excess above the Standard Model expectations must be viewed taking into account the number of such channels a fluctuation could have occurred in. However, since we are repeating a published analysis, we are now in a position that the signature has been chosen and the cuts have been set *a* *priori* so that we can calculate the statistical probability of getting a specific result. So initially we have set the Run II selection criteria to be the same as for Run I, so as to make a direct repeat of the Run I analysis but with substantially more data. We will in parallel optimize a new analysis that exploits the new features of the upgraded CDF-II detector.

2 The CDF Detector

The description of the CDF Detector and information about the upgrades for the Run II has been published elsewhere [12], [13], [14].

Those changes to the CDF Detector from Run I to Run II that are particularly relevant to this analysis are:

- Improved Muon System Coverage. The azimuthal areas near the top and bottom of the detector previously without coverage in the central region have been substantially filled in. A new system, the IMU system, covers the region $1.0 < |\eta| < 1.5$ with a 4-layer barrel of drift tubes (the BMU system) and scintillators (the WSU, BSU, and TSU systems).

- The previous 'plug' and 'forward' calorimeters that used multi-wire proportional chambers and that covered the region $1.1 < |\eta| < 4.2$ have been replaced by new scintillator-based 'plug' calorimeters that cover $1.1 < |\eta| < 3.6$.

- The tracking system has been improved. The new central drift chamber has a smaller cell size and hence a shorter drift time, and has an additional 12 extra layers of sense wires for a total of 96 measurements on a track that traverses the whole chamber. An expanded SVX detector system, now 90-cm long with one single–sided layer and six double–sided layers in the central region, and an additional layer at larger η, adds more points to central tracks and extends tracking measurements for electron identification, for example, out to a rapidity of 2.5.

- More Passive Material. The improved silicon system, however, means more material for photon conversion to e^+e^- pairs, and larger radiation by electrons.

Each of these changes some details of the analysis from that of Run I, but implies no major change in how one deals with either signal or backgrounds.

In addition, the selection of triggers is different, particularly with regard to muons. However, the effects of the trigger changes on this analysis, which selects high-p_T leptons and photons, are minimal, as the efficiencies are still high for the triggers we use.

3 Selection of Photon-Lepton Candidates

3.1 Datasets

Photon-lepton candidates are obtained from the top group 'tight-remake' electron and muon samples [15], which have been ntupled using the UC flat ntuple [16].

The ntuple dataset locations are listed at **http://hep.uchicago.edu/cdf/datasets/.**

The electron samples are located on the UC cluster at:
/cdf/data10a/Datasets/non_express/electron/UCntuples/4.11.2_lepton.
The electron dataset contains a total of 1119664 events.

The muon samples are are located on the UC cluster at:
/cdf/data10a/Datasets/non_express/muon/UCntuples/4.11.2_lepton.
The muon dataset contains a total of 272002 events.

3.2 Good Run Selection

Because of the present situation of having a substantial fraction of the data without the SVX or without the CMX being operational, we use two standard EWK good run definitions. The more inclusive list is called 'Partial Detector' below.

The second good run selection, called 'Full Detector' below, is a subset of Partial Detector list and requires two additional data quality bits to be set, SVX_STATUS and CMX_OFFLINE. The good run bits for Partial Detector and for the Full Detector are summarized in Table 1.

Bit	Partial Detector	Full Detector
GOODRUN_STATUS	1	1
CAL_STATUS	1	1
CMU_STATUS	1	1
CMP_STATUS	1	1
COT_STATUS	1	1
CAL_OFFLINE	1	1
CMU_OFFLINE	1	1
CMP_OFFLINE	1	1
COT_OFFLINE	1	1
B0INTEGRATEDLIVELUMI > 10	1	1
CMX_OFFLINE	any	1
SVX_STATUS	any	1

Table 1: Good run bits for the Partial Detector and for the Full Detector

3.3 Luminosity

We get the luminosity using the utilities **luminosityLog** and **lumsum.pl** on the official luminosity page [17]. The total luminosity is 193 pb^{-1} for the 'Partial' detector sample.

3.4 Muon Identification

We require at least one 'tight central muon' in a event for it to be classified as a muon-photon event. In both electron-photon and muon-photon events we search for additional muons using a definition of 'loose central muon'. We describe these two sets of cuts below.

3.4.1 Tight Central Muons

The muon selection criteria for a tight central muon are listed in Table 2 and are described below. Tight central muons are identified by extrapolating tracks in the COT through the calorimeters, and the extrapolation is required to match to a stub either in both the CMU and CMP muon detectors (a 'CMUP' muon), or in the CMX system. Tight central muons are required to have a track-stub matching distance less than 3 cm for CMU, less than 5 cm for CMP, and less than 6 cm for CMX. The definition of a tight muon in addition requires the track to extrapolate to the fiducial region of the relevant detector system (both CMU and CMP for CMUP muons, CMX for CMX muons). In the current analysis we use only CMUP muons as tight muons, and will use both CMUP and CMX tight muons for the 5.3 analysis.

These cuts are identical to those used by the Top Group [18] for the Generation 4 releases, with the exception that we have not applied the impact parameter cut, and have added two additional cuts that will be applied in Generation 5 that remove decays-in-flight [19]. The impact parameter calculation uses the default muon track rather than the parent COT track, and in the Top Group selection a tighter cut is applied if the track does in fact contain silicon hits. Instead, we have tabulated this d_0 cut for reference but we do not use it to select tight (Table 2) or loose muons (Table 3). The two additional cuts reject charged kaon decays in flight in which a low-momentum kaon ($\sim$ 5 GeV, typically) decays inside the COT with the kaon and decay-muon tracks forming a 'seagull' pattern which is reconstructed as a single high-momentum track. These tracks often remove a complete stereo layer in order to get a good fit, and are badly mis-reconstructed in polar angle. They consequently often are recorded to leave zero energy in the extrapolated traversed calorimeter towers [20].

The muon tracks used in the initial selection for this analysis are beam-constrained COT-only,

Variable	Cut	Cumulative	N-1	This Cut
no cuts (note: V1.1)		296867	0	296867
Track P_t	$> 25\ GeV$	160043	0	160043
Track quality cuts	3x3SLx7 hits	138821	2453	254100
Track quality cuts	Chi2/(N of COT hits-5) < 3	136849	148	285282
$\|z0\|$	$< 60\ cm$	136742	1	295514
Calorimeter Energy (Em)	$< 2 + max(0, 0.0115 * (p - 100))\ GeV$	135177	109	268606
Calorimeter Energy (Had)	$< 6 + max(0, 0.028 * (p - 100))\ GeV$	134786	48	278855
Cal.Energy (EM+Had)	> 0.1 GeV	133594	28	289557
Fractional Calorimeter Isolation E_T	< 0.1	114621	10634	169144
CMU stub	True	70445	851	155634
$\|dX\ \ cmu\|$	$< 3\ cm$	70162	144	285786
CMP stub	True	68894	1007	149708
$\|dX\ \ cmp\|$	$< 5\ cm$	68772	71	290028
Cosmic	False	64050	4103	268043
$Track\ \|d0\|$	< 0.02 cm (si hits) OR < 0.2 cm (no si hits)	64033	17	281782

Table 2: Tight Central Muon Identification and Isolation Cuts. The selection criteria applied to the top Remake sample to make the muon sample of tight central CMUP muons. Each entry corresponds to a muon in the CDF Muon Collection, including stubless muons. The d_0 cut is not applied to select muons, but is tabulated for reference and to see its effect. The column labeled 'Cumulative' gives the effect of each successive cut on the number of muon candidates in the 272002 events in the muon subsample; the numbers in the 'N-1' column represent number of muon candidates that pass all except the cut in that row. The heading 'This Cut' represents the effect of applying only the cut listed.

as is done by the muon group in their efficiency studies [19]. For default muon tracks that contain silicon we link backwards to the COT-only parent track and use that track for all subsequent analysis. Muon tracks that have silicon hits and those that do not form two distinctly different samples, with different backgrounds [20], and different resolutions; this technique, while losing valuable information from the silicon at this stage, puts all prompt COT tracks on the same footing (however tracks with impact parameter, such as those from very high-momentum tau decay, would be much better treated using the silicon).

For tracks that are COT-only beam-constrained tracks, we also apply a curvature correction for the track p_T in data before applying kinematic selection criteria and calculating additional kinematic variables. The form of the curvature correction is shown in Equation 1 where Q is a charge of track(+1 for positive charge and -1 for tracks negative charge):

$$p_T = Q/(Q/p_T - 0.00042 - 0.00116 * sin(\phi + 0.3))) \tag{1}$$

The $\eta - \phi$ distributions are shown in Figure 2 for all muons in the sample and for those that pass the loose muon identification cuts of Table 3.

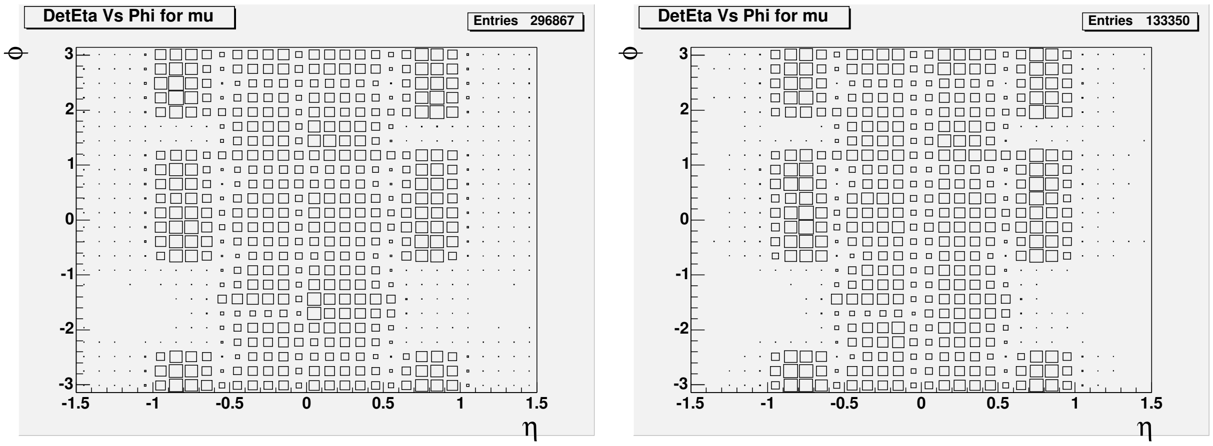

(a) $\eta - \phi$ distribution for all muon candidates

(b) $\eta - \phi$ distribution for the muons which pass loose muon identification cuts

Figure 2: (a) The $\eta - \phi$ distribution for all muon candidates and (b) for the muons which pass loose muon identification cuts, listed in Table 3.

All central muons are required to have $|z_0| < 60\ cm$ so that the collision is well-contained within the CDF detector. In order to be well-measured, the muon track is required to have minimum of 3 axial and 3 stereo superlayers with at least 7 hits in each superlayer. In addition, in order to reject kaon decays in flight that are mis-reconstructed as high momentum muons, we require at least some energy in the calorimeter towers that the muon extrapolates to, EM+Ehad > 0.1 GeV, and a good fit to the COT track, Chisq/(Number of COT hits-5) < 3 [20, 19].

High energy muons are typically isolated 'minimum-ionizing' particles that have limited calorimeter energy. A muon traversing the central electromagnetic calorimeter(CEM) deposits an average energy of ~ 0.3 GeV. Therefore we require muon candidates to deposit less than 2 GeV total in the CEM towers (we take into account two towers in the CEM) the muon track intersects. Similarly, muons transversing the central hadronic calorimeter(CHA) deposit an average energy of ~ 2

GeV; we consequently require muon candidates to deposit a total energy less than $\sim$ 6 GeV, also increasing with muon momentum, in the CHA towers intersected by the track extrapolation. To take into account the (slow) growth of energy loss with momentum, for very high energy muons ($p > 100\ GeV$) we require the measured CEM energy to be less than $2.0 + 0.0115 * (p - 100)\ GeV$ and CHA energy to be less than $6.0 + 0.028 * (p - 100)\ GeV$.

To suppress hadrons and decay muons created from hadrons in jets we require the total transverse energy deposited in the calorimeters in a cone of R=0.4 around the muon track direction(known as the fractional calorimeter isolation E_T) to be less than 0.1 of the muon track pt.

To suppress cosmic rays we use CosmicFinderModule [21, 22] and reject events which tagged as Cosmic Ray muons. To be more specific, if bit "0" of the bit mask for which CosmicFinderModule cuts fail is equal to 1, this is a cosmic ray and the event is rejected.

3.4.2 Loose Central Muons

While each muon-photon event has to contain at least one tight muon, both electron-photon and muon-photon events are searched for additional high-p_T muons that could come from the decays of heavy particles. The cuts for these additional muons, described in Table 3, are looser than the tight cuts, and in particular do not require a stub in the muon chambers. Including these 'stubless muons', there are four types of additional muons:

- CMU muons (muon track matches the CMU stub only);
- CMP muons (muon track matches a stub in the CMP only;
- CMX muons (muon track matches a stub in the CMX only.
- CMIO muons (muon track doesn't match any stub).

Track P_t	$> 20\ GeV$
$\|z0\|$	$< 60\ cm$
Calorimeter Energy (Em)	$< 2 + max(0, 0.0115 * (p - 100))\quad GeV$
Calorimeter Energy (Had)	$< 6 + max(0, 0.028 * (p - 100))\quad GeV$
Fractional Calorimeter Isolation E_t	< 0.1
Track quality cuts	3x3SLx7 hits

Table 3: Identification and Isolation Cuts for Additional Muons

3.4.3 Muon Control Sample

The W and Z^0 provide control samples for the lepton-photon samples. We use data triggered by the MUON_CMUP_18 trigger for both Z^0 and W candidates. .

The selection criteria for the $Z^0 \to \mu^+\mu^-$ control sample are listed in Table 6. We require two muons in the event. One must pass the tight cuts (Table 2), and another must pass the loose cuts (Table 3). We further require the two muons to have opposite charge, and require the difference of the z_0 beam-line coordinates of the muon tracks to be less than 4 cm. The last requirement for counting Z^0 events is that the invariant mass of the muon pair of the Z^0 candidate should be between 66 GeV and 116 GeV. We find 4325 Z^0 events. We also find 4 same-sign 'Z^0' events, indicative of the level of tracking problems. The selection variable distributions for the $Z^0 \to \mu^+\mu^-$ control sample are shown in Figure 3.

The selection criteria for the $W^{\pm} \to \mu^{\pm}\nu$ control sample are listed in Table 5. We require one tight muon (i.e. $p_T > 20$), and corrected missing E_T greater than 25 GeV. We require the transverse mass of the W candidate to be in the mass window 30-120 GeV. To reject $Z^0 \to \mu^+\mu^-$ events in which one muon is not identified, events with a second track with $p_T > 10$ GeV and associated EM and HAD calorimeter energies less than 3 and 9 GeV, respectively, are rejected. We find 47871 $W^{\pm} \to \mu^{\pm}\nu$ events, 23849 positive and 24022 negative W's. The $W^{\pm} \to \mu^{\pm}\nu$ mass, p_T, and $\Delta\phi$ distributions are shown in Figure 4.

Category	N
Events with at least one Tight Muon	62513
Tight Muons	63410
Tight + Loose Muons	4614
$Z^0 \to \mu^+\mu^-$(triggered+M_Z window cut)	4325
$W^{\pm} \to \mu^{\pm}\nu$(triggered+M_W window cut)	47871

Table 4: A summary of the numbers for the muon control samples. Muon cuts are listed in Table 2, $Z^0 \to \mu^+\mu^-$ cuts in Table 6, and $W^{\pm} \to \mu^{\pm}\nu$ cuts in Table 5

Variable	Cut
Tight Muon	Cuts are listed in Table 2
Missing E_T Cut	$E_T > 25$ GeV
Z-Rejection	No 2nd Track with $P_T > 10$ GeV, $E_{EM} < 3$ GeV, and $E_{HAD} < 9$ GeV
Mass Window Cut	$M_T > 30$ GeV and < 120 GeV
Trigger	MUON_CMUP_18

Table 5: $W^{\pm} \to \mu^{\pm}\nu$ Selection Cuts

Variable	Cut
Tight Muon	Cuts are listed in Table 2
Loose Muon	Cuts are listed in Table 3
Muon tracks must be of opposite charge	$Q^{\mu 1} + Q^{\mu 2} = 0$
Delta Z cut	$\lvert Z^{\mu 1}_{TRACK}$ - $Z^{\mu 2}_{TRACK}\rvert < 4$ cm
Mass Window cut	$M > 66$ GeV and < 116 GeV
Trigger	MUON_CMUP_18

Table 6: $Z^0 \to \mu^+\mu^-$ Selection Cuts. Superscripts $\mu 1$ and $\mu 2$ stand for muons in the event

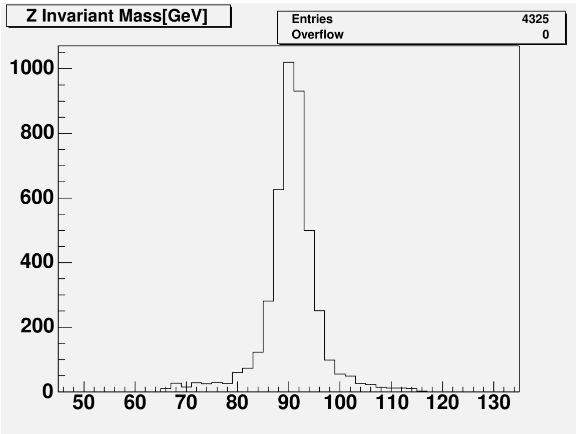

(a) Invariant Mass

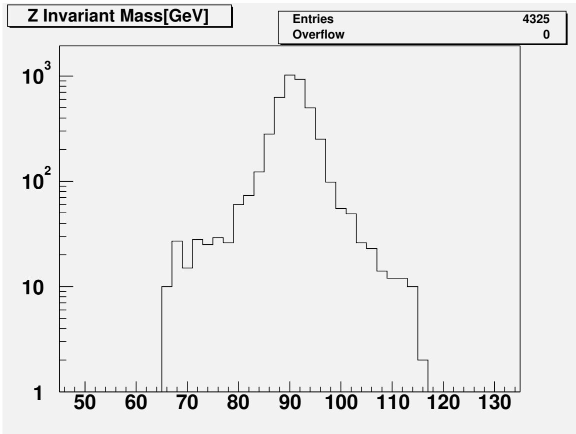

(b) Invariant Mass (log)

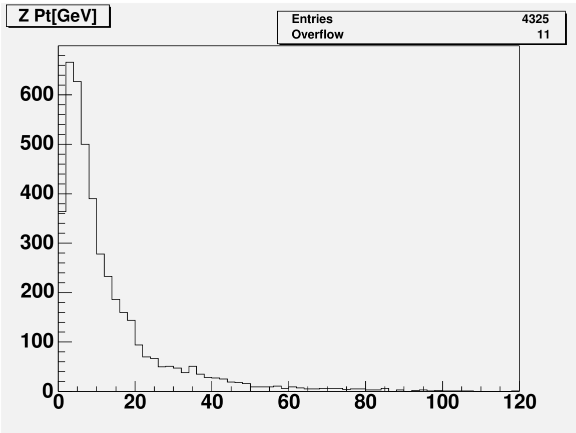

(c) P_T of $Z^0 \to \mu^+\mu^-$

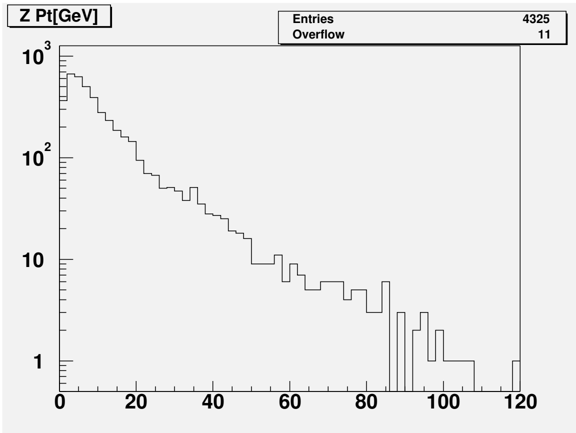

(d) P_T of $Z^0 \to \mu^+\mu^-$ (log)

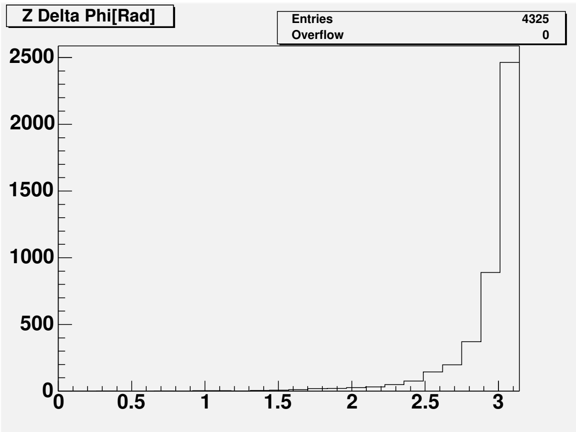

(e) $\Delta\phi$ of $Z^0 \to \mu^+\mu^-$

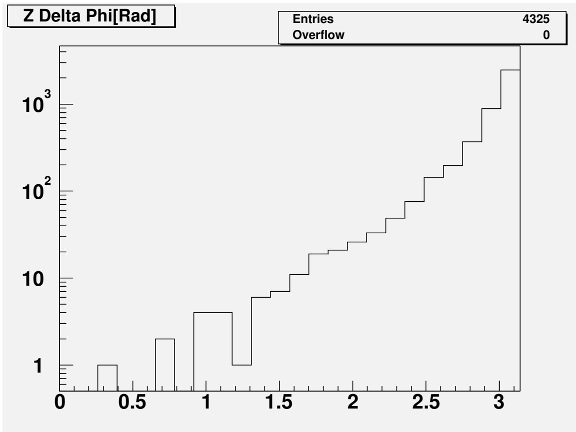

(f) $\Delta\phi$ of $Z^0 \to \mu^+\mu^-$ (log)

Figure 3: The distributions for Invariant Mass of $Z^0 \to \mu^+\mu^-$, P_T of $Z^0 \to \mu^+\mu^-$, $\Delta\phi$ of $Z^0 \to \mu^+\mu^-$, linear plots(a, c, e), log plots(b, d, f). The histogram is $Z^0 \to \mu^+\mu^-$ candidates.

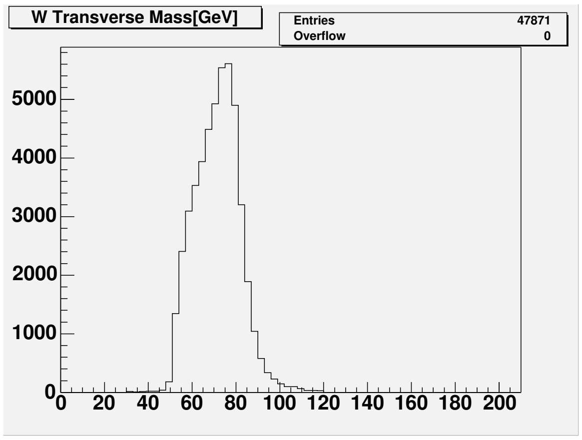

(a) Transverse Mass

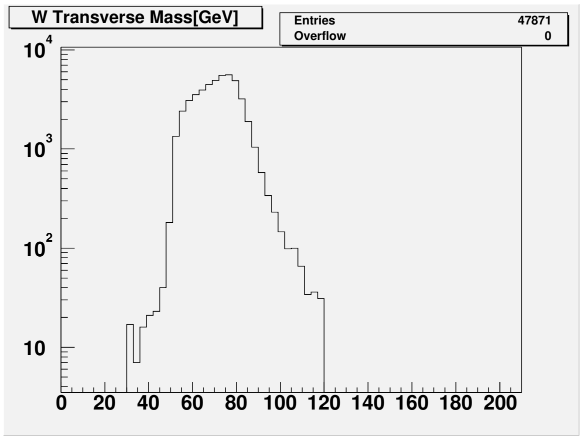

(b) Transverse Mass (log)

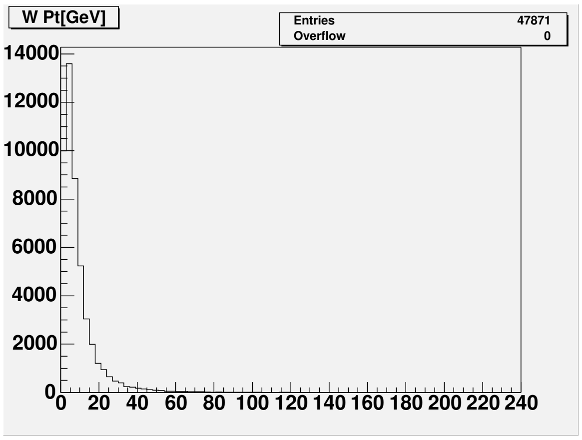

(c) P_T of $W^{\pm} \to \mu^{\pm}\nu$

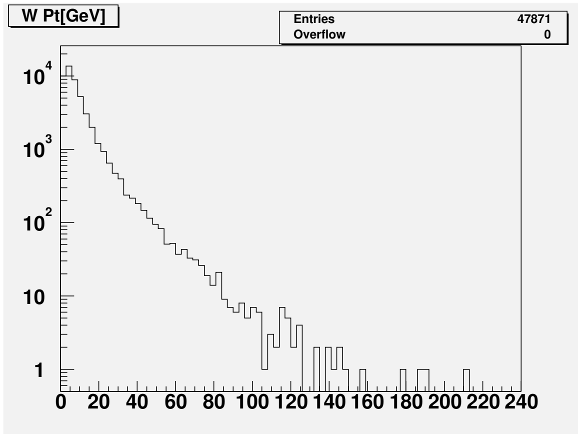

(d) P_T of $W^{\pm} \to \mu^{\pm}\nu$ (log)

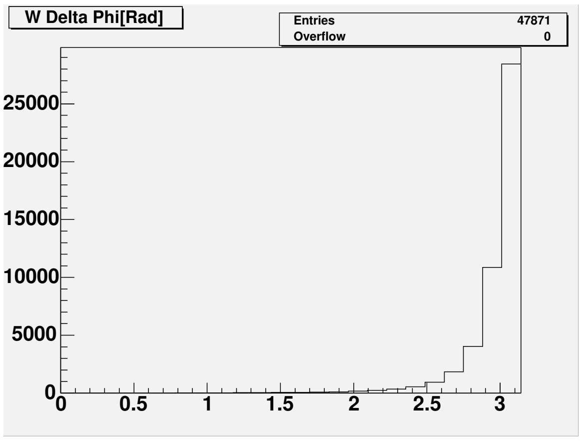

(e) $\Delta\phi$ of $W^{\pm} \to \mu^{\pm}\nu$

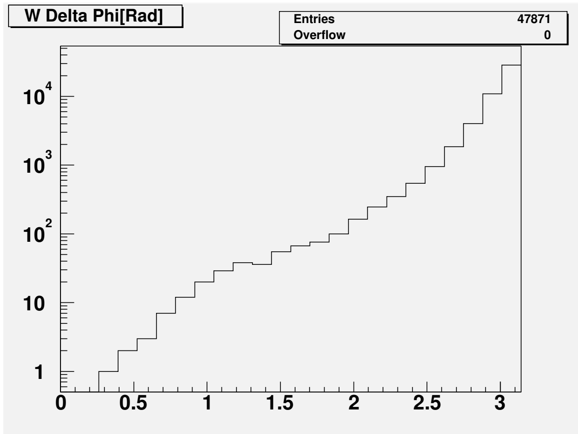

(f) $\Delta\phi$ of $W^{\pm} \to \mu^{\pm}\nu$ (log)

Figure 4: The distributions for Transverse Mass of $W^{\pm} \to \mu^{\pm}\nu$, P_T of $W^{\pm} \to \mu^{\pm}\nu$, $\Delta\phi$ of $W^{\pm} \to \mu^{\pm}\nu$, linear plots(a, c, e), log plots(b, d, f)

3.5 Electron Identification

We require at least one 'tight central electron' in a event for it to be classified as a electron-photon event. In both electron-photon and muon-photon events we search for additional 'loose' electrons in the CEM and PEM. We describe the tight central and loose central and plug cuts below.

3.5.1 Tight Central Electrons

The selection criteria for tight central electrons are listed in Table 7 and are described below.

Electrons are identified in the CEM by matching high momentum tracks to high-energy CEM clusters. The electron track is the highest momentum track which intersects one of two towers in the CEM cluster. The electron tracks that we use in this analysis are beam-constrained COT-only. We apply the same corrections to the electron tracks as we do to the muon tracks.

The selection cuts are the same as those used in the measurements of the W and Z crossections [23] and [24] with exception for fiducial requirement(see below).

An electron candidate is required to have tracking momentum (p) which exceeds half of its calorimeter energy (E). The electron track is required to have a minimum of 3 axial and 3 stereo SL segments containing at least 7 hits each. In order that the momentum resolution doesn't make for inefficiencies for very high-energy electrons, for $E_t > 50\ GeV$ the E/p cut is not applied (leaving only the the $\mathrm{p_T} > 10$ GeV cut as the requirement on the track). The electrons are required to have the track extrapolate to the beam line within $|Z_0| < 60\ cm$ so that CDF detector contains

Variable	Cut	Cumulative	N-1	This Cut
no cuts (note: v1.0)		1606313	0	1606313
E_T	$> 25\ GeV$	462250	0	462250
Track P_t	$> 10\ GeV$	454010	53	929995
Track $\|z0\|$	$< 60\ cm$	453965	15	1599349
Had/Em	$< 0.055 + 0.00045 * E$	451990	71	1366319
E/P (for $E_T < 50GeV$ only)	< 2.0	429801	8277	1126009
Lshr	< 0.2	429007	129	1134596
Chi2 Strips	< 10	427586	645	1458698
charge-signed $DeltaX$	-3.0 cm $< Q_{trk} * deltaX <$ 1.5 cm	427407	79	1138021
$\|DeltaZ\|$	$< 3.0\ cm$	424126	842	1116409
Fractional Calorimeter Isolation E_T	$< 0.1\ GeV$	294266	104717	535243
Track quality cuts	3x3SLx7 hits	280973	11789	1189425
Fiducial	$Ces\|X\| < 21\ cm$, $9\ cm < Ces\|Z\| < 230\ cm$	257391	23582	1403496

Table 7: Tight Central Electron Identification and Isolation Cuts. The initial selection is that for the top Remake sample. Each entry corresponds to Cdf Central Em Object. The column labeled 'Cumulative' gives the effect of each successive cut on the number of electron candidates in the 1119664 events in the electron subsample; the numbers in the 'N-1' column represent number of electron candidates that pass all except the cut in that row. The heading 'This Cut' represents the effect of applying only the cut listed.

the collision well.

The position of the track extrapolated to the CES radius must satisfy the following requirements: it must fall within charge-signed CES shower position of the cluster in the r-phi view $DeltaX - 3.0\ cm\ <\ Q_{trk} * \Delta_X\ <\ 1.5\ cm$ and it must fall within 3 cm of the CES shower position in the Z-direction(Δ_Z).

The CEM shower characteristics should be consistent with that of a single charged particle. We require the ratio of the total energy of the CHA towers located behind the CEM towers in the electron cluster to that of the electron itself to be less than than 0.055+0.00045*E GeV. A comparison of the lateral shower sharing with neighboring towers in the CEM cluster with test-beam data is parameterized by a dimensionless quantity, L_{shr}, which must have a value less than 0.2.

We require the χ^2 for the profile of energy deposited in the CES strips compared to that expected from test beam data to be less than 10. No χ^2 cut is made on the profile in the CES wires as bremsstrahlung will separate from the electron in the $r\phi$ view.

As additional isolation requirement, the total transverse energy deposited in the calorimeter in a cone R=0.4 around the electron track, must be less than 0.1 of the E_t of the electron. The isolation is corrected via the standard algorithm [25], for leakage, but not the number of vertices.

To ensure that events are well-measured the shower position of the electron is required to fall within the fiducial region of the CES so that the shower is fully contained in the active region.

For this we require $Ces|X|\ <\ 21$ cm, $9\ <\ Ces|Z|\ <\ 230$ cm, and we exclude the 'chimney' region, $0.82\ <\ \eta_{detector}\ <\ 1.1$ and $(\pi/2\ <\ \phi\ <\ 5\pi/12$. We use this fiducial requirement for both tight (Table 7) and loose (Table 8) electrons.

We apply no rejection against photon conversions producing electrons at this point in the analysis; this will be done in the 5.3 samples.

3.5.2 Loose Central Electrons

While each electron-photon event has to contain at least one tight electron, both electron-photon and muon-photon events are searched for additional high-p_T electrons that could come from the decays of heavy particles. The cuts for these additional electrons, described in Table 8, are looser than the tight cuts, and in particular do not require any of the CES variables, i.e. no track-cluster match in Δx or Δz and no cut on strip χ^2, and also no cut on Lshr.

E_t	$> 20\ GeV$
Track P_t	$> 10\ GeV$
Track $\|z0\|$	$< 60\ cm$
Had/Em	$< 0.055 + 0.00045 * E$
E/P (for $E_t\ <\ 50\ GeV$ only)	< 2.0
Fractional Calorimeter Isolation E_t	< 0.1
Track quality cuts	3x3SLx7 hits
Fiducial	$Ces\|X\| < 21\ cm$, $9 < Ces\|Z\| < 230\ cm$

Table 8: Identification and Isolation Cuts for Loose Central Electrons. These criteria are used to select 'additional' central electrons in events with either a tight electron or tight muon.

3.5.3 Plug Electrons

Additional isolated electrons in the plug calorimeter with $E_T > 15$ GeV are identified for measured PES rapidities of $1.2 < |\eta| < 2.5$. Each entry corresponds to Cdf Plug Em Object. The cuts used for plug electron identification are given in Table 9. We require minimal leakage or activity in the hadron calorimeter, $Had/Em < 0.05$, a fractional isolation (isolation energy over the electron energy) less than 0.1, and the shower shape to satisfy the the Pem 3x3 χ^2 and Pes5over9 5-strip to 9 strip ratio cuts.

Variable	Cut	Cumulative	N-1	This Cut
no cuts (note: v1.0)		219881	0	219881
E_T	$> 15\ GeV$	39320	0	39320
Had/Em	< 0.05	22063	684	136593
Fractional Calorimeter Isolation E_T	$< 0.1\ GeV$	15540	565	63418
Chi2 Strips	< 10	12770	1946	64530
PES 5by9 u and v	> 0.65	11921	287	91394
PES $\|\eta\|$	$> 1.2\ ,\ < 2.8$	10761	1160	100686

Table 9: Identification and Isolation Cuts for Additional Plug Electrons

3.5.4 Electron Control Sample

As in the muon case, the W and Z^0 provide control samples for the electron-photon samples. We require at least one tight electron pass the ELECTRON_CENTRAL_18 trigger for both W and Z^0 candidates, where tight electrons are the electrons that pass the cuts in Table 7.

The selection criteria for the $Z^0 \to e^+e^-$ central-central control sample are listed in Table 11. For this sample a Z^0 candidate is required to have two central electrons, one passing the tight cuts(Table 7), and the other the loose cuts (Table 8). The mass of the Z candidate is required to be within the window 66 GeV to 116 GeV. The difference in the z_0 coordinates of the two electron tracks must be less than 4 cm. We find 4935 opposite-sign events and 91 same-sign central-central Z^0 events satisfying these criteria (the large number of same sign events in the electron sample but not the muon sample is presumably due to photon conversions). The distributions in mass, p_T of the pair, and delta-phi are shown in Figure 5. We also form a central-plug dielectron Z^0

Variable	Cut
Tight Electron	Cuts are listed in Table 7
Missing E_T Cut	$E_T > 25$ GeV
Mass Window Cut	$M_T > 30$ GeV and < 120 GeV
Trigger	ELECTRON_CENTRAL_18

Table 10: $W^\pm \to e^\pm\nu$ Selection Cuts

control sample to monitor the plug electron identification performance. We require a tight central electron, and a plug electron passing the cuts of Table 9. The mass of the Z candidate is required to be within the window 66 GeV to 116 GeV. We find 3366 (3596) central-plug Z^0 events satisfying these criteria with the plug electron in the East (West) calorimeter. The distributions in mass, p_T

Variable	Cut
Tight Electron	Cuts are listed in Table 7
Loose Electron	Cuts are listed in Table 8
Electron tracks must be of opposite charge	$Q^{e1} + Q^{e2} = 0$
Delta Z cut	$\|Z^{e1}_{TRACK}$ - $Z^{e2}_{TRACK}\| < 4$ cm
Mass Window cut	$M > 66$ GeV and < 116 GeV
Trigger	ELECTRON_CENTRAL_18

Table 11: $Z^0 \rightarrow e^+e^-$ Selection Cuts. Superscripts $e1$ and $e2$ stand for electrons in the event

of the pair, and delta-phi are shown in Figure 6. The selection criteria for the $W^\pm \rightarrow e^\pm\nu$ control sample are listed in Table 10. We require one tight central electron (i.e. $p_T > 20$), and corrected missing E_T greater than 25 GeV. We require the transverse mass of the W candidate to be in the mass window 30-120 GeV. We find 47871 $W^\pm \rightarrow \mu^\pm\nu$ events, 23849 positive and 24022 negative W's. The $W^\pm \rightarrow \mu^\pm\nu$ mass, p_T, and $\Delta\phi$ distributions are shown in Figure 4.

Category	N
Events with at least one Tight Electron	248673
Tight Electrons	252677
Tight + Loose Central Electron	5363
Tight + East Plug Electron	3560
Tight + West Plug Electron	3775
CC $Z^0 \rightarrow e^+e^-$(triggered+M_Z)	4935
CE Plug $Z^0 \rightarrow e^+e^-$(triggered+M_Z)	3366
CW Plug $Z^0 \rightarrow e^+e^-$(triggered+M_Z)	3596
$W^\pm \rightarrow e^\pm\nu$(triggered+$M_W$)	100153

Table 12: Control numbers for the electron sample. Electron cuts in Table 7, $Z^0 \rightarrow e^+e^-$ cuts in Table 11, $W^\pm \rightarrow e^\pm\nu$ cuts in Table 10. CC refers to Central-Central events; CE refers to Central-East Plug, CW refers to Central-West Plug.

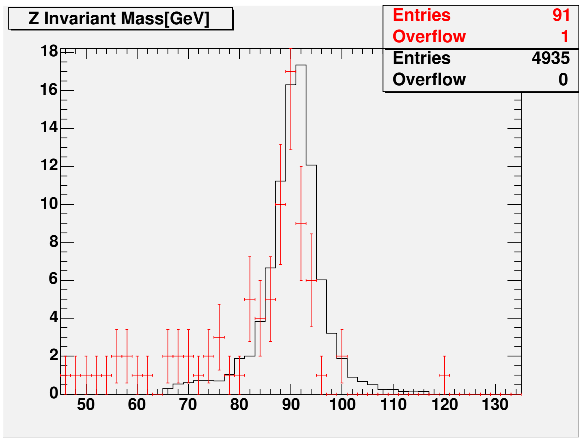

(a) Invariant Mass

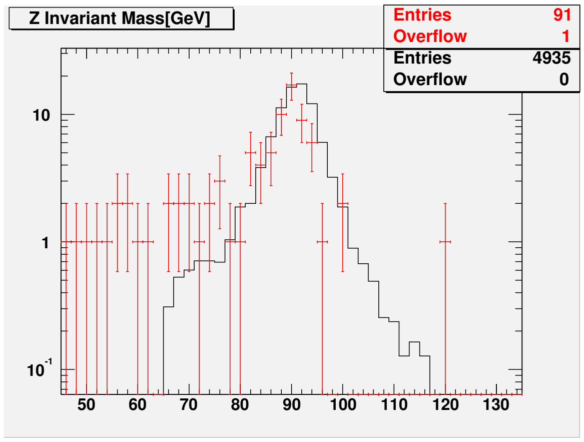

(b) Invariant Mass (log)

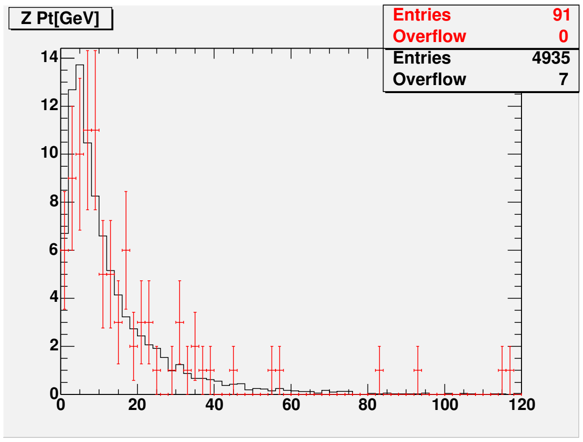

(c) P_T of $Z^0 \to e^+e^-$

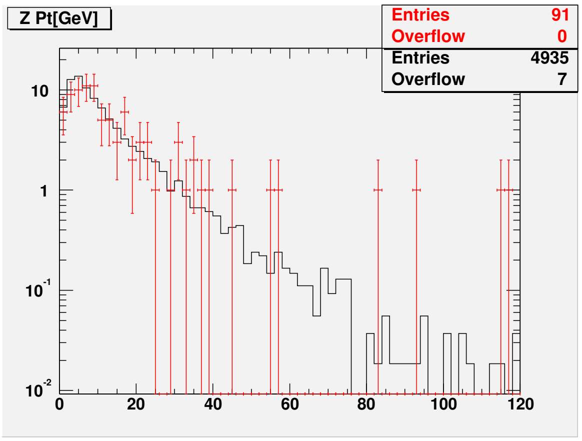

(d) P_T of $Z^0 \to e^+e^-$ (log)

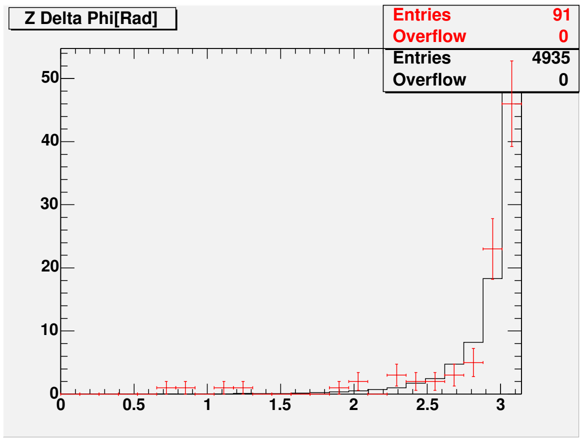

(e) $\Delta\phi$ of $Z^0 \to e^+e^-$

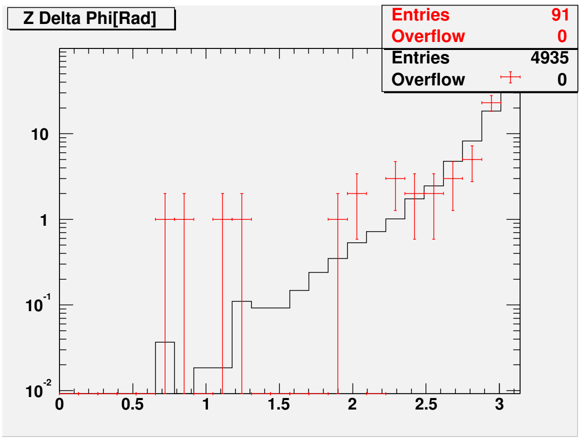

(f) $\Delta\phi$ of $Z^0 \to e^+e^-$ (log)

Figure 5: The distributions for Invariant Mass of $Z^0 \to e^+e^-$, P_T of $Z^0 \to e^+e^-$, $\Delta\phi$ of $Z^0 \to e^+e^-$, linear plots(a, c, e), log plots(b, d, f). The histogram is $Z^0 \to e^+e^-$ candidates. The red points are events with same sign electrons.

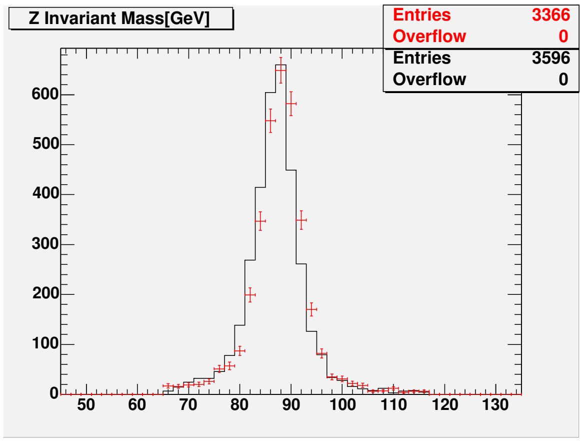

(a) Invariant Mass

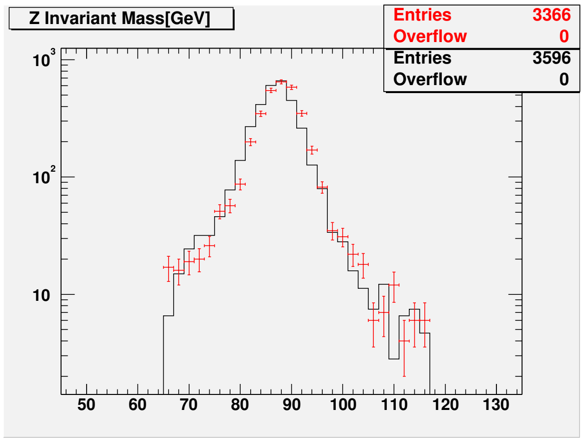

(b) Invariant Mass

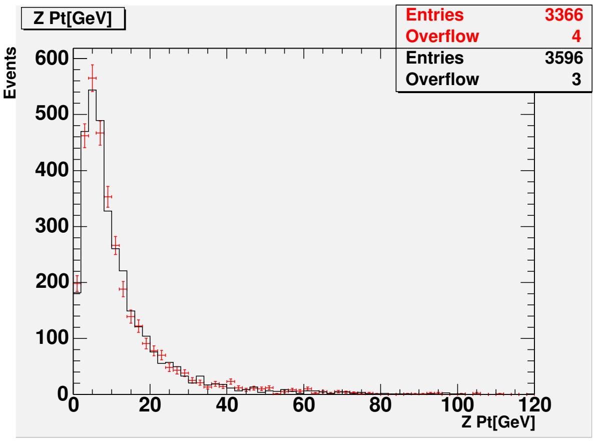

(c) P_T of $\mathrm{Z}^0 \to e^+e^-$

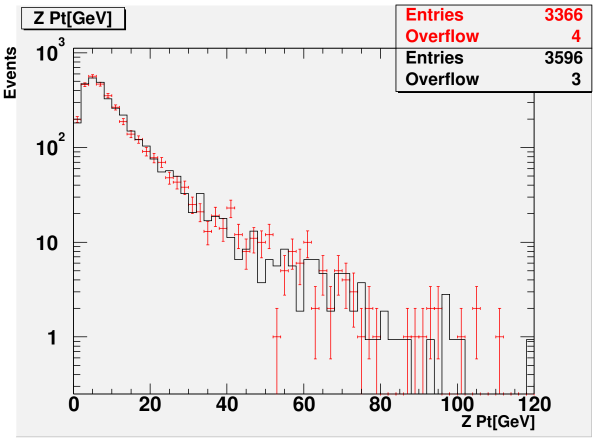

(d) P_T of $\mathrm{Z}^0 \to e^+e^-$

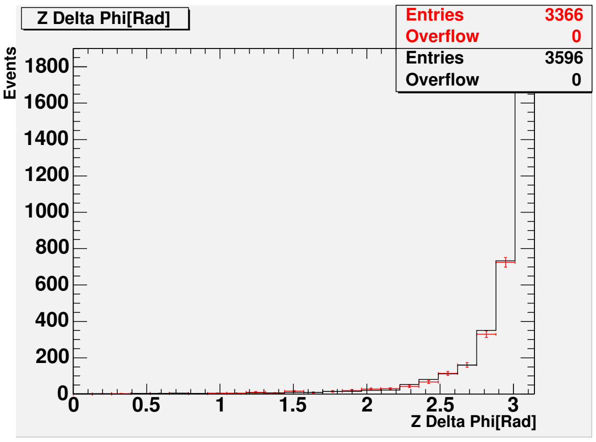

(e) $\Delta\phi$ of $\mathrm{Z}^0 \to e^+e^-$

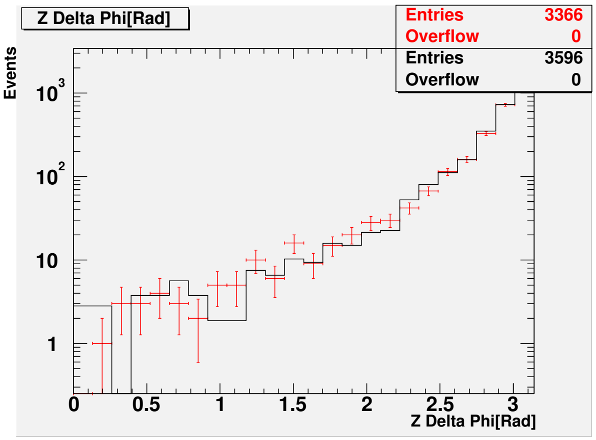

(f) $\Delta\phi$ of $\mathrm{Z}^0 \to e^+e^-$

Figure 6: Central-plug dielectron $\mathrm{Z}^0 \to e^+e^-$ control sample to monitor the plug electron identification performance. We require a tight central electron(Table 7), and a plug electron passing the cuts of Table 9. The distributions for Invariant Mass of $\mathrm{Z}^0 \to e^+e^-$, P_T of $\mathrm{Z}^0 \to e^+e^-$, $\Delta\phi$ of $\mathrm{Z}^0 \to e^+e^-$, linear plots(a, c, e), log plots(b, d, f). We find 3366 (3596) central-plug Z^0 events satisfying these criteria with the plug electron in the East (West) calorimeter. The points are Central-East Plug $\mathrm{Z}^0 \to e^+e^-$ candidates; the histogram is Central-West Plug $\mathrm{Z}^0 \to e^+e^-$ candidates.

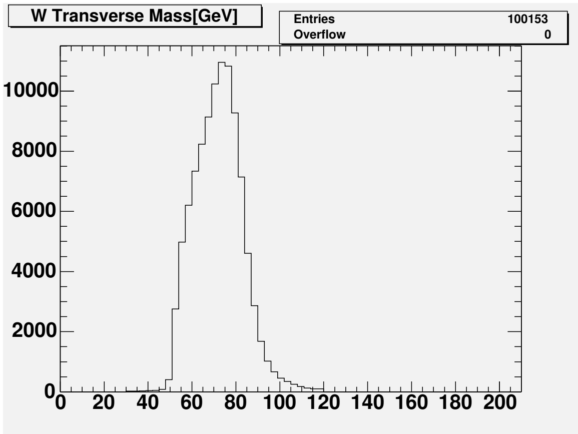

(a) Transverse Mass

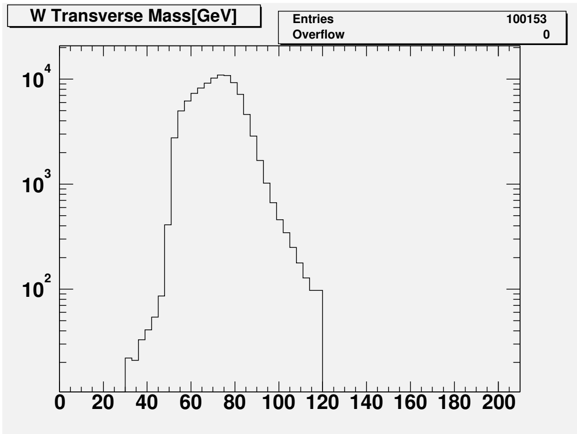

(b) Transverse Mass (log)

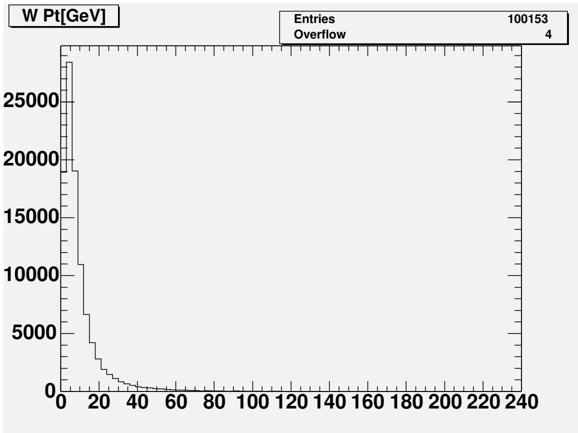

(c) P_T of $\mathrm{W}^\pm \to e^\pm \nu$

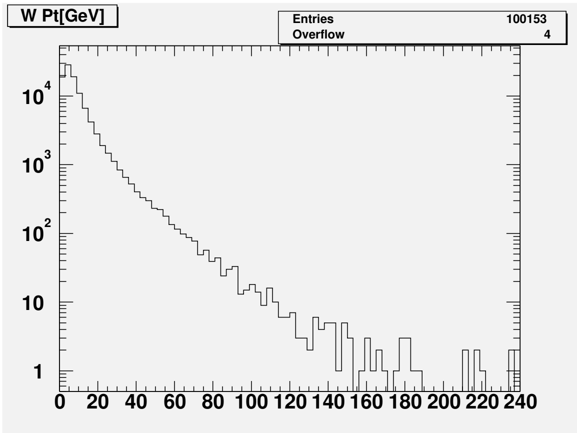

(d) P_T of $\mathrm{W}^\pm \to e^\pm \nu$ (log)

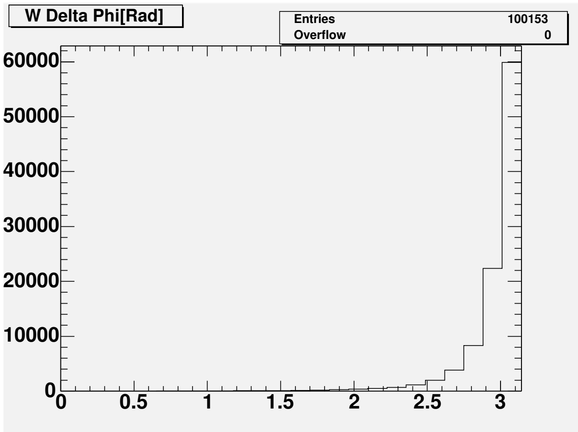

(e) $\Delta\phi$ of $\mathrm{W}^\pm \to e^\pm \nu$

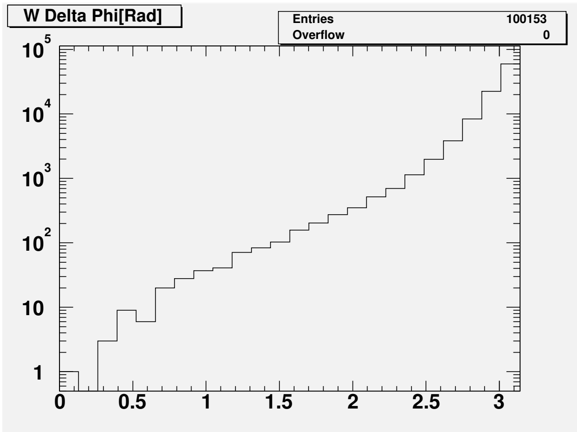

(f) $\Delta\phi$ of $\mathrm{W}^\pm \to e^\pm \nu$ (log)

Figure 7: The distributions for Transverse Mass of $\mathrm{W}^\pm \to e^\pm \nu$, P_T of $\mathrm{W}^\pm \to e^\pm \nu$, $\Delta\phi$ of $\mathrm{W}^\pm \to e^\pm \nu$, linear plots(a, c, e), log plots(b, d, f).

3.6 Photon Identification

The photon selection criteria are identical for the muon and electron samples; the cuts, and the number of events passing in each sample, are enumerated in Tables 13, 14 and are described below.

The photon candidate is required to have corrected transverse energy greater than 25 GeV. For photons or electrons the CES shower position is determined by the energy-weighted centroid of the highest energy clusters of those strips and wires in the CES which correspond to the seed tower. The photon's direction is determined by the line connecting the primary event vertex to the shower position in the CES.

To ensure that events are well measured the shower position of the photon is required to fall within the fiducial region of the CES so that the shower is fully contained in the active region.

Photon candidates are required to have characteristics consistent with those of a neutral electromagnetically interacting particle. No COT track with $p_t > 1\ GeV$ may point at the photon cluster. One track with $p_t < 1\ GeV$ may point at the cluster.

IsoE_T^{corr} is the Run I cone 0.4 isolation energy with the Run I correction to isolation energy due to phi-crack leakage [25]. TrackIso is a track isolation in a cone 0.4

3.6.1 Photons in the Muon Subsample

Table 13 summarizes the selection of photons in the muon sample. We find a total of 27 events with both a tight muon and a photon satisfying the above cuts.

Variable	Cut	Cumulative	N-1	This Cut
no cuts (note: V1.0)		151278	0	151278
E_T^{corr}	$> 25\ GeV$	3335	0	3335
Had/Em	$< 0.055 + 0.00045 * E^{corr}$	1672	1	101383
χ^2 $(Strips + Wires)$ / 2.0	< 20	463	3	84554
N Track	$<= 1$	286	2	109333
Track P_t	$< 1 + 0.005 * E_T^{corr}\ \ GeV$	177	5	75947
$Cone0.4$ IsoE_T^{corr}	$< 2.0 + 0.005 * E_T^{corr}$	97	16	52068
$Cone0.4$ TrackIso	$< 5.0 + 0.005 * E_T^{corr}$	80	13	71422
2nd CES cluster (strip and wire)	$< 2.4 + 0.01 * E_T^{corr}$	77	2	134249
Fiducial	$Ces\|X\| < 21\ cm$, $9\ cm < Ces\|Z\| < 230\ cm$	72	5	89617

Table 13: Photon Identification and Isolation Cuts for the Muon Subsample. Each entry corresponds to Cdf Em Object, Central or Plug. The total number of Cdf Em Objects is the same for electrons and photons as expected. The column labeled 'Cumulative' gives the effect of each successive cut on the number of photon candidates in the 272002 events in the muon subsample; the numbers in the 'N-1' column represent number of photon candidates that pass all except the cut in that row. The heading 'This Cut' represents the effect of applying only the one cut listed.

3.6.2 Photons in the Electron Subsample

Table 14 summarizes the selection of photons in the electron sample. We find a total of 249 events with both a tight electron and a photon satisfying the above cuts. Note the disparity between this number and the 27 muon-photon events; this is due to a number of causes, as discussed later.

Variable	Cut	Cumulative	N-1	This Cut
no cuts (note: V1.0)		1826194	0	1826194
E_T^{corr}	$> 25\ GeV$	479723	0	479723
Had/Em	$< 0.055 + 0.00045 * E^{corr}$	470880	6	1537485
$\chi^2\ (Strips + Wires)\ /\ 2.0$	< 20	373051	63	1279930
N Track	<= 1	193575	9	1051876
Track P_t	$< 1 + 0.005 * E_T^{corr}\quad GeV$	1186	443	428502
$Cone0.4$ IsoE_T^{corr}	$< 2.0 + 0.005 * E_T^{corr}$	616	158	726696
$Cone0.4$ TrackIso	$< 5.0 + 0.005 * E_T^{corr}$	589	17	374851
2nd CES cluster (strip and wire)	$< 2.4 + 0.01 * E_T^{corr}$	546	41	1561179
Fiducial	$Ces\|X\| < 21\ cm$, $9\ cm < Ces\|Z\| < 230\ cm$	505	41	1401428

Table 14: Photon Identification and Isolation Cuts for the Electron Subsample. The column labeled 'Cumulative' gives the effect of each successive cut on the number of photon candidates in the 1119664 events in the electron subsample; the numbers in the 'N-1' column represent number of photon candidates that pass all except the cut in that row. The heading 'This Cut' represents the effect of applying only the one cut listed.

3.6.3 Photon Control Sample

The dominant source of fake background for photon-electron events is $Z^0 \to e^+e^-$ production, wherein one of the electrons undergoes hard photon bremsstrahlung in the detector material, or the COT fails to detect one of the electron tracks, and that electron subsequently passes all of the photon cuts. There are approximately 4002 central electron pairs in the CDF data, so a photon fake rate as low as 1% will give rise to 80 photon-electron background events, which would be unacceptably high for finding sources of new physics comparable to $W/Z^0 + \gamma$ production

A control sample of Z^0-like events is selected from the 204 two-body photon-electron candidates (See Section 5) by requiring that the invariant mass of the photon-electron pair, $M_{e\gamma}$, be within 10 GeV (or 5 GeV, like in Run I [11]) GeV of the Z^0 mass (91 GeV). There are 97 (73) such events in the CDF data, and their characteristics are shown in Figure 8 (these figures are for candidates within 10 GeV of the Z^0 mass. It is observed that the shapes of the distributions of the two samples ($Z^0 \to e^+e^-$ and $Z \to e`\gamma`$) are similar to each other(Figure 9).

3.7 Missing $\mathrm{E_T}$ Identification

Missing Et is calculated from the CdfMet object. The vertex used to calculate the $\not{E}_T$ is the primary vertex, in this case the vertex with the largest attached $\mathrm{p_T}$. The $\not{E}_T$ is then corrected for different objects.

We apply all corrections from the ucntuple for the met in electron sample but corrections for CMIO muons and jets. For this we take all corrections for the met for the electron sample from the ntuple, which corresponds to photons with $\mathrm{E_T} > 25GeV$, central and plug electrons with $\mathrm{E_T} > 12GeV$.

In the muon subsample we correct met only for loose muons with $\mathrm{E_T} > 20GeV$.

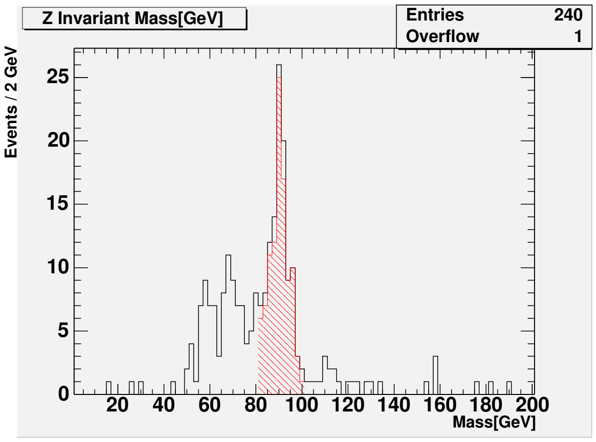

(a) $Z \to e`\gamma`$ Invariant Mass

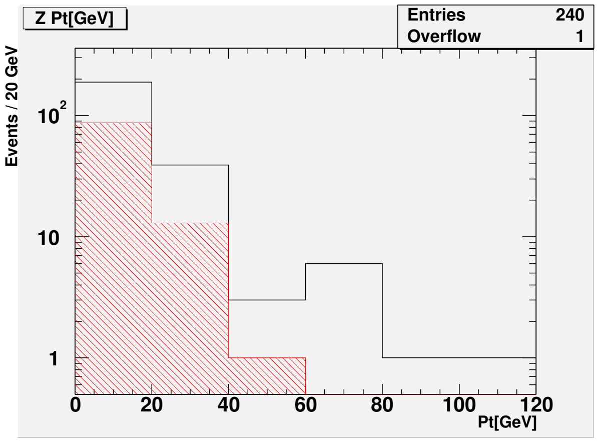

(b) Pt of $Z \to e`\gamma`$

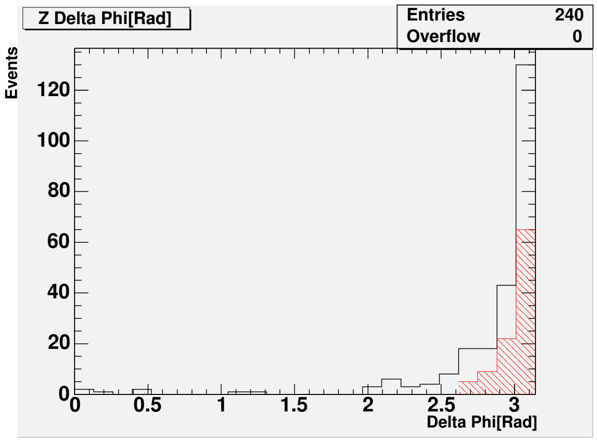

(c) $\Delta\phi$ of $Z \to e`\gamma`$

Figure 8: Photon Control Sample: (a) $Z \to e`\gamma`$ invariant mass; (b) p_T of $Z \to e`\gamma`$; (c) $\Delta\phi$ between e and γ; Photons from Z^0-like events are shown in red.

In 5.3 we plan to correct met for each of the objects that is specifically identified in this analysis, i.e. tight and loose electrons with $\mathrm{E_T} > 8$ GeV, tight and loose muons with $\mathrm{p_T} > 8$ GeV, and photons with $\mathrm{E_T} > 8$ GeV. In addition the $\not{E}_\mathrm{T}$ will be corrected for jets with $\mathrm{E_T} > 8$ GeV at Level 5.

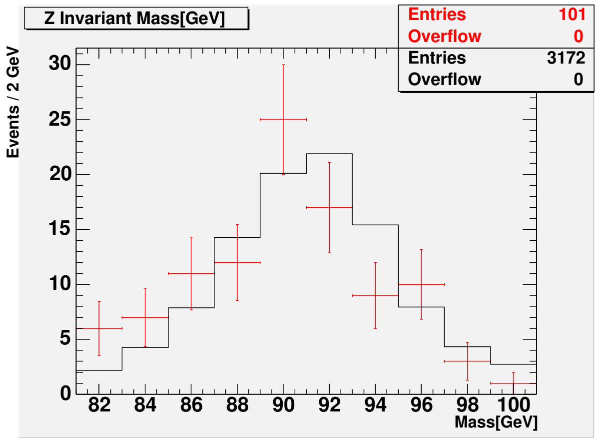

(a) Invariant Mass

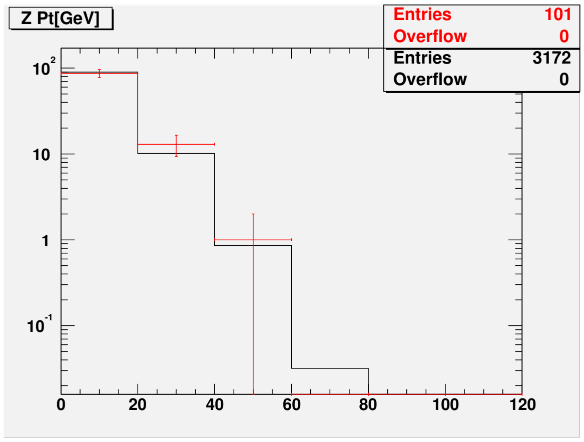

(b) p_T of Z^0

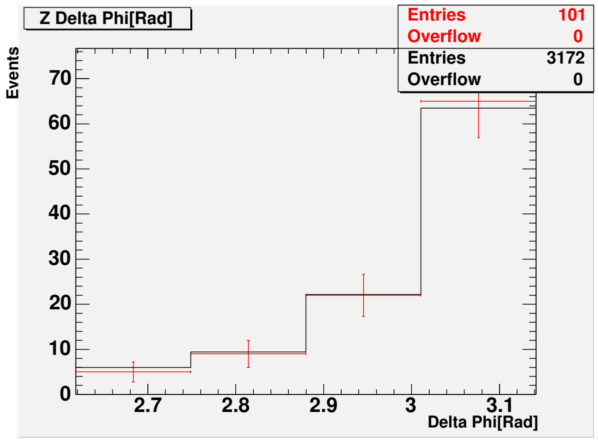

(c) $\Delta\phi$

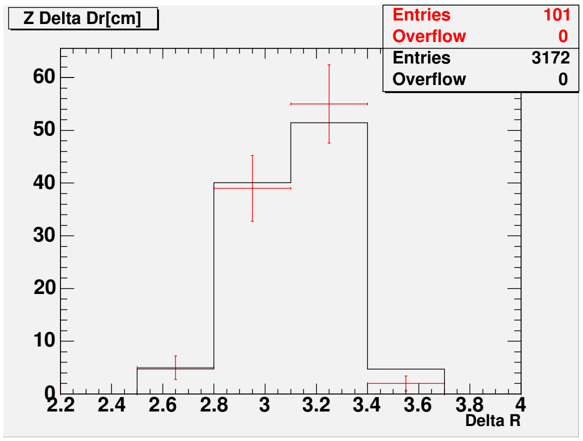

(d) ΔR

Figure 9: The distributions for: (a) Invariant Mass of $Z \to e`\gamma`$, (b) p_T of $Z \to e`\gamma`$, (c) $\Delta\phi$ of $Z \to e`\gamma`$, (d) ΔR of $Z \to e`\gamma`$. The points are the Z^0-like photon-electron sample; the shaded histogram is electron-electron events from CDF data with the same kinematic cuts, normalized to the number of events in the control sample.

3.8 Criteria for Additional Objects In the Event

Our analysis includes investigating of the associated production of other photons, leptons, jets and large missing E_T in events containing high E_T lepton and high E_T photon. Identification of the additional leptons is less selective as the presence of the primary photon and lepton is a good signature which reduces the sources of the misidentified particles.

Identification of the additional photons are the same as that for the primary one.

4 Standard Model Predictions

4.1 Introduction: The Matrix Element Generators

The dominant source of photon-lepton events at the Tevatron is electroweak diboson production, in which an electroweak boson (W or Z^0) decays leptonically ($\ell\nu$ or $\ell\ell$) and a photon is radiated from either an initial state quark, a charged electroweak boson (W), or a final state lepton. The number of photon-lepton events from electroweak diboson production is estimated using several leading-order (LO) Monte Carlo event generator programs. These programs are MadGraph [26], [27], CompHep [28], and Baur [29].

These programs output 4-vectors and helicities of particles emanating from a diboson production event in an ASCII format. These files are then fed into the LesHouchesModule [30], which runs Pythia to add parton fragmentation and final-state radiation and initial-state radiation (both QED and QCD) , and then writes out the events in CDF HEPG format. These files are then used as input to the CDF detector simulation program. This program outputs simulated data in a format identical to that of an actual CDF Run II event. Simulated photon-lepton event rates can then be estimated in a manner identical to that of CDF data.

4.2 Checks

4.2.1 Comparison of different samples at GENERATOR and HEPG levels

To be highly confident in the SM predictions, we compared the predictions from the three independent LO matrix-element generators. The MadGraph and CompHep samples had been previously compared at GENERATOR level in [31]. The Baur samples were created separately [32]. We have performed additional comparisons for variables at the HEPG level for MadGraph, Baur, and CompHep. These are shown in Figures 10, 11, 12, 13, where the CompHep predictions are shown in blue symbols, Madgraph in red symbols, and Baur as a black histogram. There is generally very good agreement between CompHep and MadGraph [31], with less good agreement, but adequate for the prediction we need (see the tables of the numbers of predicted events), with Baur, especially in the mass and p_T distributions for $Z^0\gamma$ samples.

We attribute these differences to differences in the generation of the samples: the Baur $Z^0\gamma$ sample has a minimum requirement of 20 GeV for a lepton-lepton mass and for a lepton-lepton-photon mass [32]; the MadGraph and CompHep samples have only a 6 GeV cut on the p_T of the photons and leptons. The MadGraph and CompHep samples, however, extend only to $|\eta \leq 2.5$, which cuts off the eta distributions. We have generated new MadGraph samples with $|\eta \leq 4.0$ and will use these for the 5.3 analysis.

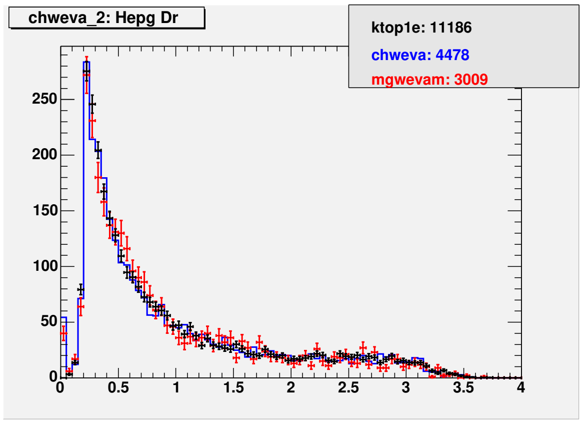

(a) Delta R between electron and photon

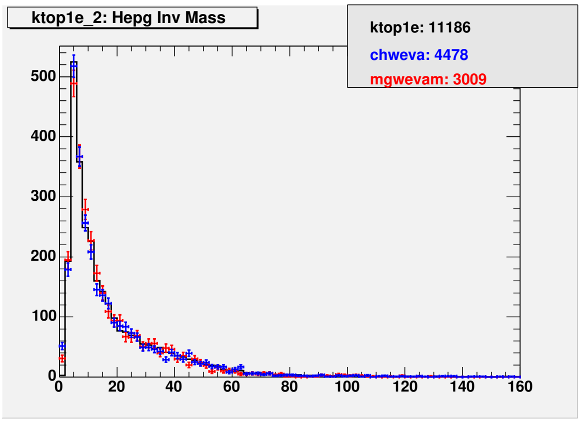

(b) Invariant mass of electron and photon

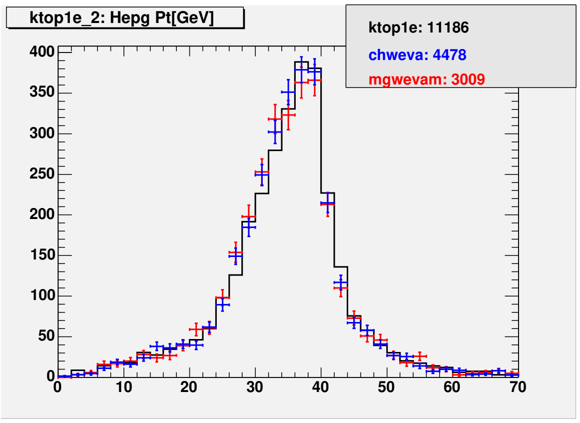

(c) Pt of 2-body (electron+photon)

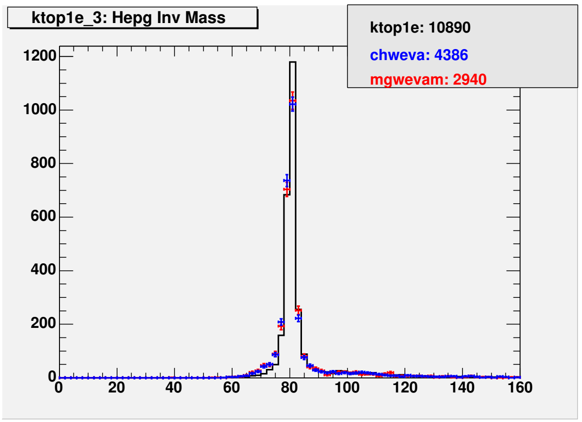

(d) Invariant mass of electron, photon and neutrino

Figure 10: The comparison at HEPG level of MadGraph (red), CompHep (blue), and Baur (black) predictions for $W\gamma$ production in the electron channel.

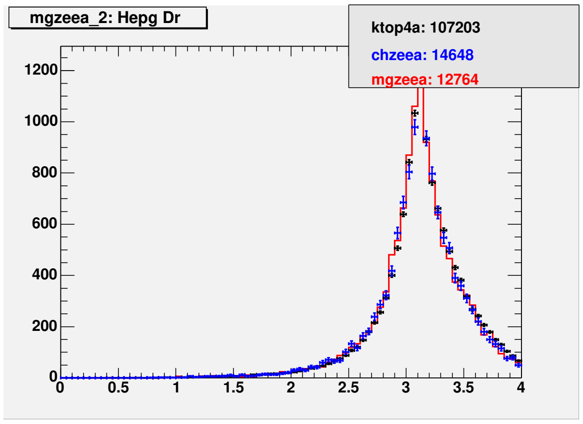

(a) Delta R between electrons

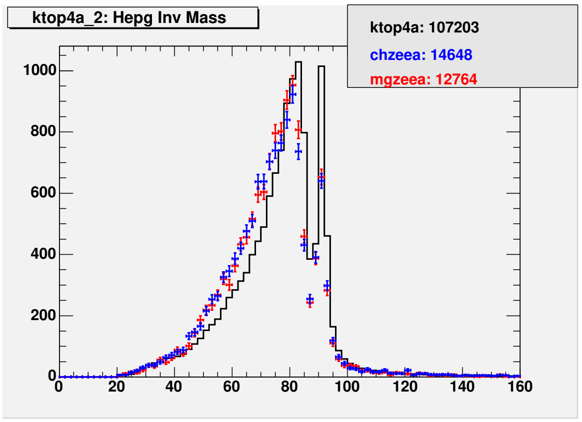

(b) Invariant mass of electrons

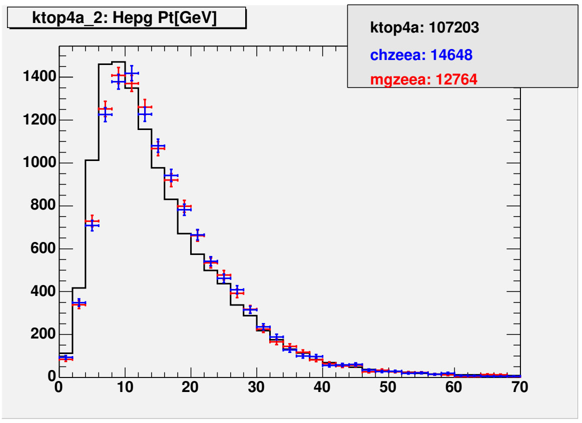

(c) Pt of 2-body(electron+electron)

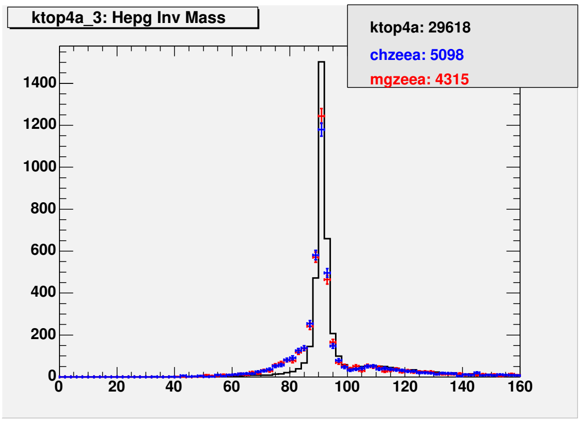

(d) Invariant mass of electron, electron and photon

Figure 11: The comparison at HEPG level of MadGraph (red), CompHep (blue), and Baur (black) predictions for $Z^0\gamma$ production in the electron channel.

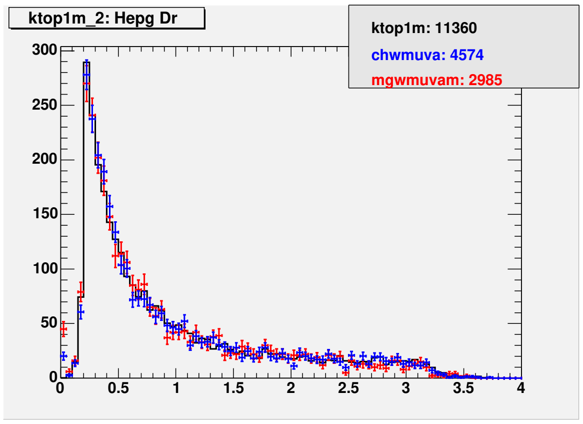

(a) Delta R between muon and photon

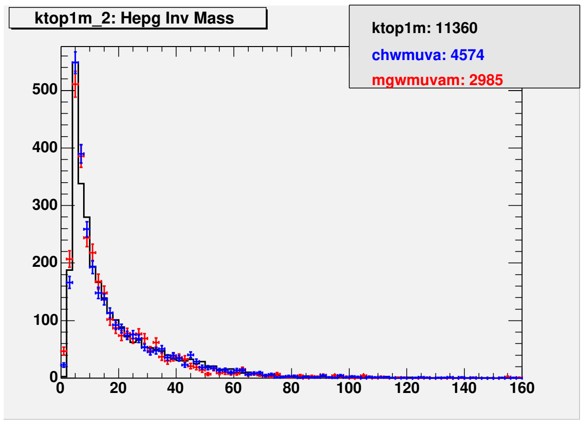

(b) Invariant mass of muon and photon

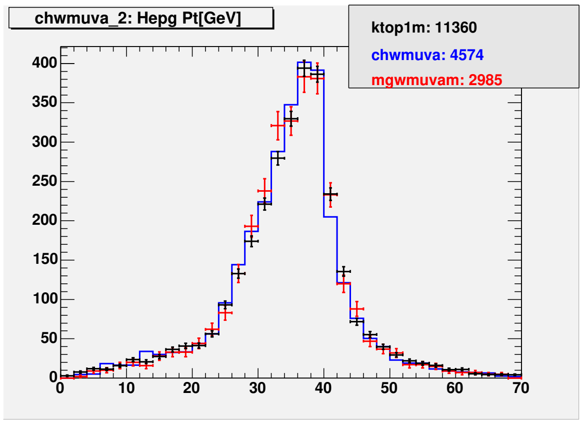

(c) Pt of 2-body (muon+photon)

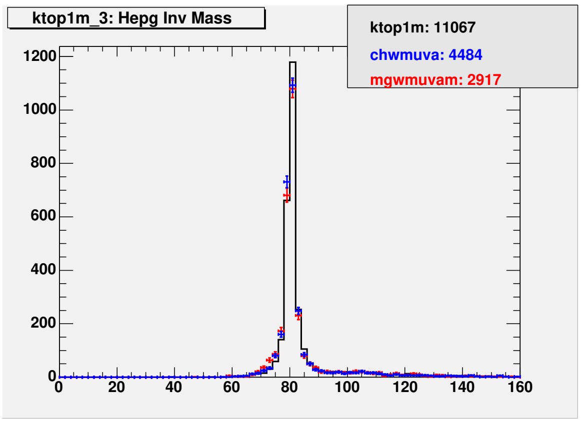

(d) Invariant mass of muon, photon and neutrino

Figure 12: The comparison at HEPG level of MadGraph (red), CompHep (blue), and Baur (black) predictions for $W\gamma$ production in the muon channel

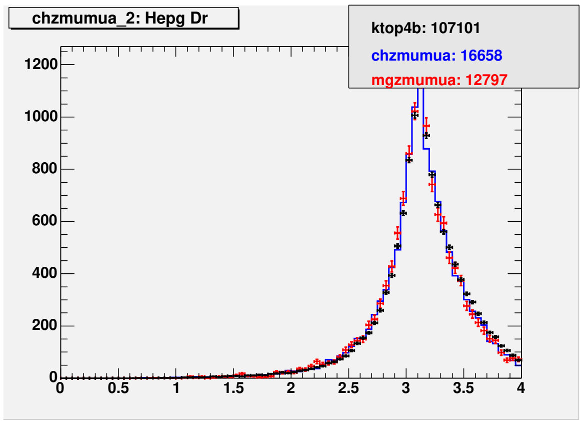

(a) Delta R between muons

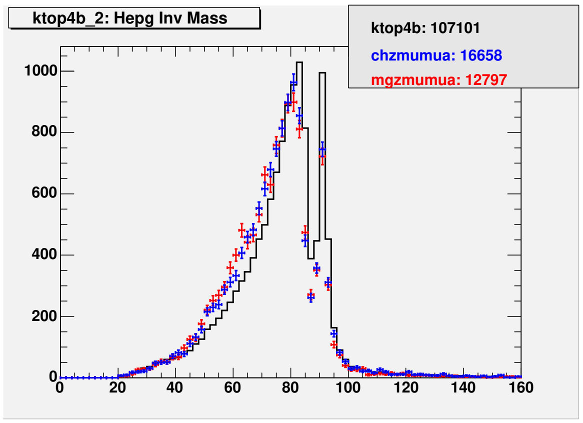

(b) Invariant mass of muons

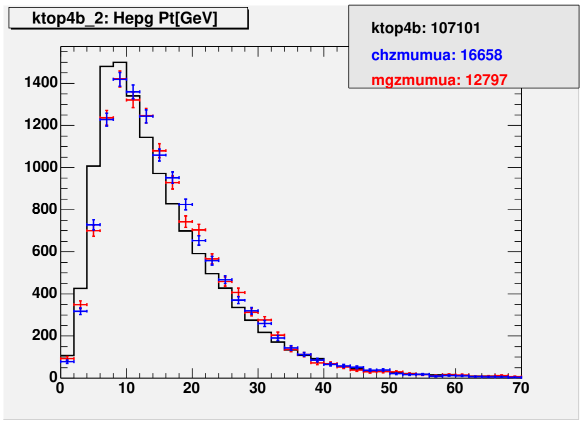

(c) Pt of 2-body(muon+muon)

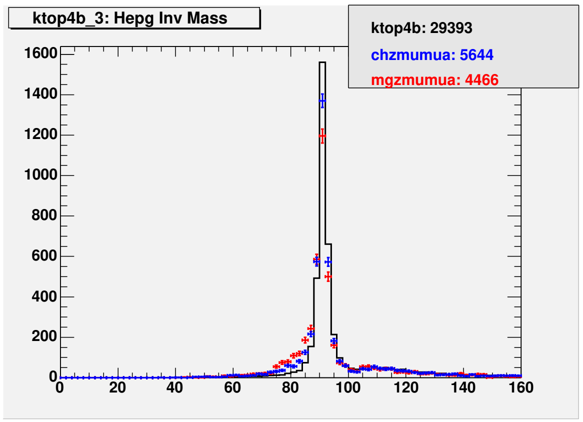

(d) Invariant mass of muon, muon and photon

Figure 13: The comparison at HEPG level of MadGraph (red), CompHep (blue), and Baur (black) predictions for $Z^0\gamma$ production in the muon channel

4.2.2 Lepton $\mathrm{E_T}$ and P_T Resolution: Comparison of HEPG and Reconstructed Values

We compare the generated value at HEPG level of $\mathrm{E_T}$ for electrons and photons, and, the value of $\mathrm{p_T}$ for muons, to the corresponding reconstructed values in simulated data to check the simulation of detector resolutions and energy scales.

We define δE as difference between the transverse energy of the particle in the HEPG block and transverse energy of the reconstructed particle, $\delta E = E_T{}^{HEPG} - E_T{}^{PROD}$. We plot the distribution of $\delta E/E_T{}^{HEPG}$ in bins of $E_T{}^{PROD}$, and fit them with the gaussian $G(x) = Constant * exp(-0.5 \times [(x - mean)/sigma]^2)$. We then plot the sigmas from the fits with respect to $E_T{}^{PROD}$. Figure 14 shows the sigma from the fit versus $\mathrm{E_T}$ for electrons (left-hand plot) and versus $\mathrm{p_T}$ for muons (right-hand plot). Also shown in Figure 14 are fits to the expected forms of the resolutions, i.e. $f(x) = C_0/\sqrt{x} + C_1$ for electrons, and $f(x) = C_0 \times x + C_1$ for muons. . We find reasonable agreement with the nominal parameters for electrons ($C_0^{nom} = 13.5\%$ and $C_1^{nom} \simeq 1\%$) with a fitted stochastic term $C_0 = 0.153 \pm 0.018\%$ and a constant term $C_1 = 0.008 \pm 0.003\%$. The fitted muon $\mathrm{p_T}$ resolutions are in good agreement with expectations at $C_0 = 0.00094 \pm 6e - 05\%$ and $C_1 = 0.004 \pm 0.002\%$. We conclude that the simulation of the calorimeter energy resolution for central electrons and the tracking momentum resolution for central muons is behaving as expected.

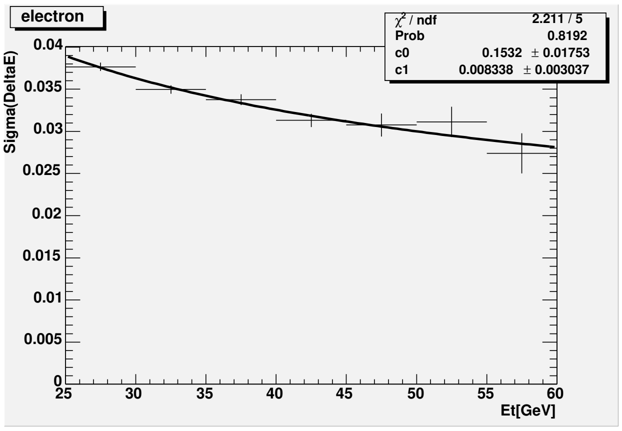

(a) Electrons from WenuA Baur sample

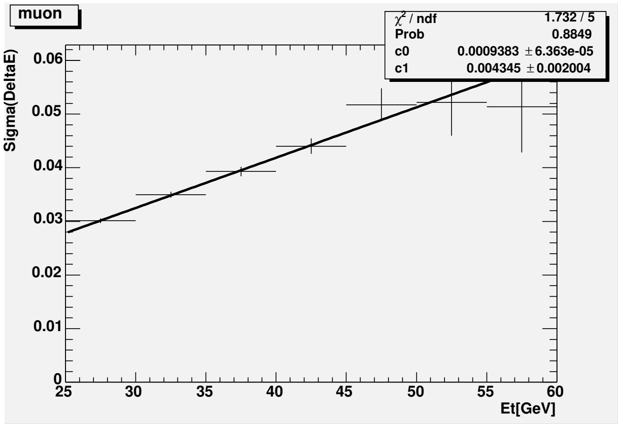

(b) Muons from WmunuA Baur sample

Figure 14: The fitted resolution in the difference between the values from HEPG and from after PRODUCTION for $\mathrm{E_T}$ for electrons (left) and $\mathrm{p_T}$ for muons (right) from the electron-photon and muon-photon samples, respectively. The resolution at each $\mathrm{E_T}$ ($\mathrm{p_T}$) is determined by fitting a Gaussian to $\delta E_T = E_T{}^{HEPG} - E_T{}^{PROD}$ (electrons) or $\delta P_T = P_T{}^{HEPG} - P_T{}^{PROD}$(muons) versus $E_T{}^{PROD}(P_T{}^{PROD})$.

Figure 15 shows the similar exercise for photons from the electron sample (left) and muon sample (right). The agreement is less good for photons than for electrons: for photons in the electron sample we get $C_0 = 0.1844 \pm 0.036\%$ and a constant term $C_1 = 0.004 \pm 0.006\%$, and in the muon sample $C_0 = 0.211 \pm 0.033\%$ and a constant term $C_1 = -0.001 \pm 0.005\%$ [33], where we expect $C_0^{nom} = 13.5\%$ and $C_1^{nom} \simeq 1\%$. This is worrying, and we will see if the effect persists in Version 5.3.3. [1]

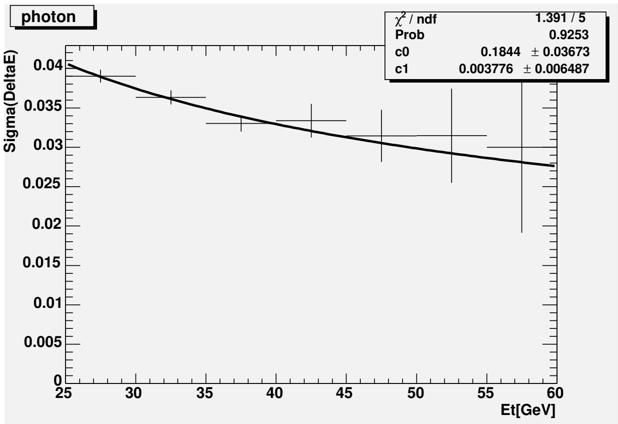

(a) Photons from WenuA Baur sample

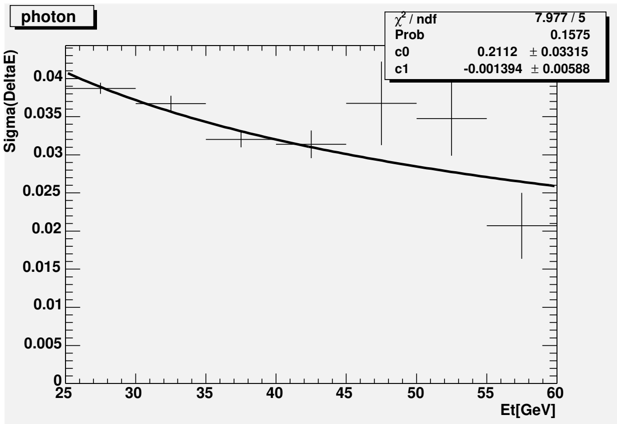

(b) Photons from WmunuA Baur sample

Figure 15: The fitted resolution in the difference between the values from HEPG and from after PRODUCTION for $\mathrm{E_T}$ for photons from the electron-photon (left) and muon-photon (right) samples, respectively. The resolution at each $\mathrm{E_T}$ ($\mathrm{p_T}$) is determined by fitting a Gaussian to $\delta E_T = {E_T}^{HEPG} - {E_T}^{PROD}$.

4.3 The SM Diboson Processes $W\gamma$ and $Z^0\gamma$ as Sources of Lepton-Photon Events

4.3.1 Expected rates from $W\gamma$

The $W\gamma$ channel is the main SM contributor to the $\ell\gamma\not\!\!E_{\mathrm{T}}$ signature with the Run I cuts. In the Run I analysis, $W\gamma$ was expected to contribute 1.93 ± 0.26 events to the $e\gamma\not\!\!E_{\mathrm{T}}$ channel, out of a total of 3.41 ± 0.34, and 1.99 ± 0.27, out of a total of 4.23 ± 0.46 for the $\mu\gamma\not\!\!E_{\mathrm{T}}$ channel. Having a reliable prediction of this signature is crucial.

There are 8 diagrams involving each of the two generations of lighter quarks that produce $W\gamma$ in LO: the four for the first generation for $W^-\gamma$ are shown in Figure 16. The photon can be radiated from the incoming quarks, from the outgoing electron, or the intermediate W. The final-state radiation from the electron is the largest contributor for a photon $\mathrm{E_T}$ cut of 6 GeV and a delta-R cut of 0.2, being 11.3 pb out of a total cross-section of 13.6 pb (the relative contributions of course depend on the kinematic cuts; for example, the FSR off of the electron and the quarks have collinear divergences). More detail on the kinematic distributions and the crossections is available in Ref [31].

[1]We remind the reader that the photon energy reconstruction unfortunately differs from that of electrons at least in the number of towers and the vertex used

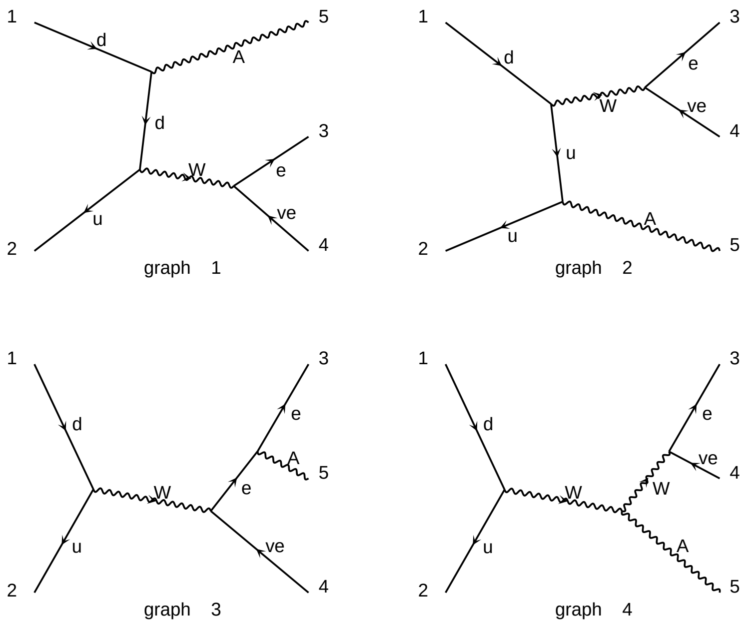

Figure 16: The LO $W\gamma$ diagrams. In MadGraph 1 and 2 are incoming particles, 3, 4, 5 are outgoing particles; 'A' designates the photon. For details on the crossection calculations see Ref [31].

Categories	*All Other*	*1 l, 1 γ, $\Delta\phi$ <150*	*$\ell\gamma\not{E}_T$*	*Multi-Lepton*	*Multi-Photon*
W-γ(MadGraph)	3.1±0.567	0.517±0.231	2.59±0.517	0±0	0±0
W-γ(CompHep)	3.39±0.48	0.0678±0.0678	3.32±0.475	0±0	0±0
W-γ(Baur)	3.64±0.332	0.486±0.121	3.16±0.31	0±0	0±0
Average	3.47±0.246	0.189±0.0573	3.08±0.232	0±0	0±0

Table 15: The predicted number of electron-photon events in xxx pb^{-1} from SM $W\gamma$ production satisfying the analysis cuts from MadGraph, CompHep and Baur. A K-factor of xxx has been applied to the LO predictions.

Categories	*All Other*	*1 l, 1 γ, $\Delta\phi$ <150*	*$\ell\gamma\not{E}_T$*	*Multi-Lepton*	*Multi-Photon*
W-γ(MadGraph)	1.44±0.384	0.411±0.205	1.03±0.325	0±0	0±0
W-γ(CompHep)	1.9±0.359	0.203±0.117	1.7±0.339	0±0	0±0
W-γ(Baur)	1.79±0.233	0.212±0.0803	1.58±0.219	0±0	0±0
Average	1.74±0.174	0.228±0.063	1.47±0.16	0±0	0±0

Table 16: The predicted number of muon-photon events in xxx pb^{-1} from SM $W\gamma$ production satisfying the analysis cuts from MadGraph, CompHep and Baur. A K-factor of xxx has been applied to the LO predictions.

The generator-level monte carlo events from MadGraph and Comphep were run through Pythia with Tune A settings and em radiation turned on. They were then run through CdfSim and 4.11.2 Production, and then ntupled [16]; a tabulation of the datasets is given in Ref. [16]. The Baur MC was ntupled from Ref. [9].

The predicted numbers of detected electron-photon events in xxx pb^{-1} from SM $W\gamma$ production satisfying the analysis cuts from MadGraph, CompHep and Baur are given in Table 15. The analogous expected rates for muon-photon events are given in in Table 16. The agreement in rates between the three monte carlos is good. We will take the average of the three as the predicted SM rate; in the 5.3.3 analysis we hope to resolve the discrepancies in the distributions (Figures 10, 11, 12, and 13), but the effects seem to be small on the rates after analysis cuts.

4.3.2 Expected Rates from $Z^0\gamma$

The process $\bar{p}p \rightarrow Z^0\gamma$ is also one of the major SM backgrounds for the lepton+ photon+X searches. It is the largest contributor to the inclusive multi-body category in the Run I search, with expected contributions in 86 pb^{-1} of 5.01 $\pm$ 0.54 events in the $e\gamma$ mode and 4.60$\pm$0.54 in the $\mu\gamma$ mode [11] It is also significant in the $\ell\gamma\not\!\!E_{\rm T}$ channel, especially for muons, as one muon can be missed inducing $\not\!\!E_{\rm T}$. The expected contributions for these the electron and muon channels in Run I were 0.32 ± 0.5 and 0.96 ± 0.15 events, respectively, smaller than the $W\gamma$ contributions, but still significant, with a total $(e + \mu)$ of 1.27 ± 0.17 out of the 7.64 ± 0.71 events expected in 86 pb^{-1}.

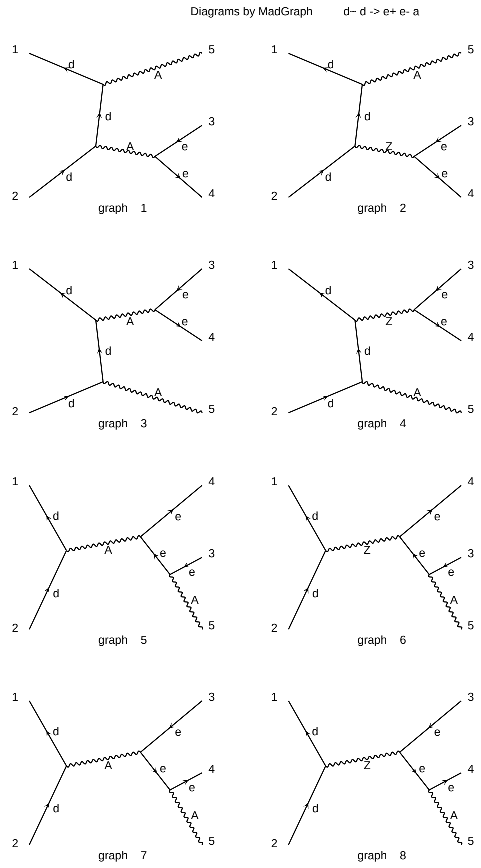

Figure 17: The LO $Z\gamma$ diagrams. In MadGraph 1 and 2 are incoming particles, 3, 4, 5 are outgoing particles; 'A' designates the photon. For details on the crossection calculations see Ref [31].

Categories	All Other	1 l, 1 γ, $\Delta\phi$ <150	$\ell\gamma\not\!\!E_T$	Multi-Lepton	Multi-Photon
Zγ(MadGraph)	9.21±0.694	3.09±0.402	1.05±0.234	5.08±0.515	0±0
Zγ(CompHep)	11.7±0.706	3.2±0.369	0.896±0.195	7.51±0.566	0.0853±0.0603
Zγ(Baur)	10.8±0.297	3.2±0.162	0.702±0.0757	6.91±0.237	0.00816±0.00816
Average	10.7±0.255	3.19±0.139	0.754±0.0676	6.71±0.201	0.00955±0.00809

Table 17: MadGraph, CompHep and Baur: $Z^0\gamma$ electron channel.

Categories	All Other	1 l, 1 γ, $\Delta\phi$ <150	$\ell\gamma\not\!\!E_T$	Multi-Lepton	Multi-Photon
Zγ(MadGraph)	4.65±0.496	0.793±0.205	1.27±0.259	2.59±0.37	0±0
Zγ(CompHep)	6.7±0.534	1.41±0.245	1.54±0.256	3.75±0.4	0±0
Zγ(Baur)	6.32±0.227	1.09±0.0945	1.5±0.111	3.72±0.174	0±0
Average	6.12±0.193	1.08±0.081	1.47±0.0948	3.55±0.147	0±0

Table 18: MadGraph, CompHep and Baur: $Z^0\gamma$ muon channel.

The predicted numbers of detected (inclusive) electron-photon events in xxx pb^{-1} from SM $Z^0\gamma$ production satisfying the analysis cuts from MadGraph, CompHep and Baur are given in Table 15. The analogous expected rates for muon-photon events are given in in Table 16. The agreement in rates between the three monte carlos is fair, with the MadGraph estimates being somewhat lower than those of CompHep and Baur. We know from CDF6057 that the generator level crossections agree between CompHep and MadGraph; for now we will take the average of the three as the predicted SM rate; in the 5.3.3 analysis we hope to resolve the discrepancies in the distributions (Figures 10, 11, 12, and 13).

4.4 The SM $W\gamma\gamma$, $Z^0\gamma\gamma$ Processes as Sources of Lepton-Photon Events

While small, the $W\gamma\gamma$, $Z^0\gamma\gamma$ processes are the largest true SM sources of a high-p_T lepton and two photons. The observation of several such events has motivated a careful study of the cross-sections for these sources [31]. In this study we have used both MadGraph and Comphep; we get excellent agreement between the two generators, giving us confidence in the predictions.

4.4.1 $W\gamma\gamma$

The final state of one lepton and two photons, $\ell\nu\gamma\gamma$, is produced in the SM through an intermediate W, with radiation off of any of the charged lines in the diagrams. The radiation from the electron produces a 'knee' in the photon E_T spectrum around 40 GeV, as the electron spectrum cuts off there. We denote the final state of $\ell\nu\gamma\gamma$ as '$W\gamma\gamma$' for convenience, although the W is virtual and the kinematics of the final state are more complicated than the name would suggest. Note that this is process has three spin-one bosons in the final state; MadGraph treats the helicities correctly (as far as we know) and writes them into the output file as input to the next steps.

The predicted numbers of detected electron-photon events in xxx pb^{-1} from SM $W\gamma\gamma$ production satisfying the analysis cuts from MadGraph and CompHep are given in Table **??**. The analogous expected rates for muon-photon events are given in in Table **??**. The agreement in rates between the two monte carlos is good. We will take the average as the predicted SM rate. More details, including kinematic distributions, can be found in Ref. [31].

Categories	*All Other*	*1 l, 1 γ, $\Delta\phi$ <150*	$\ell\gamma\not{E}_T$	*Multi-Lepton*	*Multi-Photon*
W-$\gamma\gamma$(MadGraph)	0.0282± 0.00333	0.00353± 0.00118	0.018± 0.00266	0.00627± 0.00157	0.000392± 0.000392
W-$\gamma\gamma$(CompHep)	0.0269± 0.00145	0.00218± 0.000412	0.0174± 0.00116	0.00591± 0.000678	0.00132± 0.000321
Average	0.0271± 0.00133	0.00233± 0.000389	0.0175± 0.00106	0.00597± 0.000622	0.000948± 0.000248

Table 19: The predicted number of (inclusive) electron-photon events in xxx pb^{-1} from SM $W\gamma\gamma$ production satisfying the analysis cuts from MadGraph and CompHep. A K-factor of xxx has been applied to the LO predictions.

Categories	*All Other*	*1 l, 1 γ, $\Delta\phi$ <150*	$\ell\gamma\not{E}_T$	*Multi-Lepton*	*Multi-Photon*
W-$\gamma\gamma$(MadGraph)	0.0133± 0.00229	0.00235± 0.00096	0.0106± 0.00204	0± 0	0.000392± 0.000392
W-$\gamma\gamma$(CompHep)	0.0148± 0.00107	0.00195± 0.000389	0.0121± 0.000969	7.78e-05± 7.78e-05	0.0007± 0.000233
Average	0.0145± 0.000969	0.00201± 0.000361	0.0118± 0.000875	7.78e-05± 7.78e-05	0.00062± 0.0002

Table 20: The predicted number of muon-photon events in xxx pb^{-1} from SM $W\gamma\gamma$ production satisfying the analysis cuts from MadGraph and CompHep. A K-factor of xxx has been applied to the LO predictions.

4.4.2 $Z^0\gamma\gamma$

The final state of two leptons and two photons, $\ell\bar{\ell}\gamma\gamma$, is generated through the intermediate photon and Z^0 states, with radiation off of any of the charged lines in the diagrams. We denote this as '$Z^0\gamma\gamma$' for convenience, but the two amplitudes modify the mass spectra and angular distributions, and so are both important.

This process is one of the SM mechanisms that could produce the $\mu\mu\gamma\gamma jj$ event (although with an extra two jets), and is of interest in the dilepton-diphoton searches as a background. As one can see below the SM cross sections are small, typically one femtobarn or less.

The predicted numbers of detected electron-photon events in xxx pb^{-1} from SM $Z^0\gamma\gamma$ production satisfying the analysis cuts from MadGraph and CompHep are given in Table **??**. The analogous expected rates for muon-photon events are given in in Table **??**. The agreement in rates between the two monte carlos is not bad. We will take the average as the predicted SM rate. More details, including kinematic distributions, can be found in Ref. [31].

Categories	*All Other*	*1 l, 1 γ, $\Delta\phi$ <150*	$\ell\gamma\not{E}_T$	*Multi-Lepton*	*Multi-Photon*
Z$\gamma\gamma$(MadGraph)	0.271± 0.0135	0.113± 0.00869	0.0147± 0.00314	0.135± 0.0095	0.00802± 0.00232

Table 21: MadGraph: $Z^0\gamma\gamma$ electron channel. The uncertainty in each estimate is given directly below the mean value.

Categories	*All Other*	*1 l, 1 γ, $\Delta\phi$ <150*	$\ell\gamma\not{E}_T$	*Multi-Lepton*	*Multi-Photon*
Z$\gamma\gamma$(MadGraph)	0.134± 0.00946	0.0461± 0.00555	0.0481± 0.00567	0.0381± 0.00505	0.00134± 0.000946

Table 22: MadGraph: $Z^0\gamma\gamma$ muon channel. The uncertainty in each estimate is given directly below the mean value.

4.5 Summary of $W\gamma$, $Z^0\gamma$, $W\gamma\gamma$, $Z^0\gamma\gamma$ predictions

Table 23 gives a summary of the contributions to the electron-photon and muon-photon channels from SM $W\gamma$, $Z^0\gamma$, $W\gamma\gamma$, $Z^0\gamma\gamma$ processes. We have multiplied the average LO predictions for each channel by a K-factor of xxx.

Categories	*All Other*	*1 l, 1 γ, $\Delta\phi$ <150*	$\ell\gamma\not{E}_T$	*Multi-Lepton*	*Multi-Photon*
Electron	24.49±.75	5.00±.24	9.48±.63	9.32±.27	.02648±.01146
Muon	13.28±.54	2.15±.20	6.11±.45	4.87±.19	.00351±.00140
Lepton	37.77±.91	7.15±.31	15.60±.77	14.18±.33	.02999±.01155

Table 23: Summary of $W\gamma$, $Z^0\gamma$, $W\gamma\gamma$, $Z^0\gamma\gamma$ predictions. The uncertainty in each estimate is given directly below the mean value.

4.6 Fakes

4.6.1 Jet Faking Photon

Studies of jets faking photons have been made in [34] and [35].

We use jets from our tight lepton samples to evaluate background from jets faking photons.

We take jet with weight equal to jet fake rate [34], [35], and count lepton-'fake photon' candidates in the same way as we do for real photons to calculate background for each subcategory (Table 24).

We take error on the predicted number to be 35%.

To better evaluate errors we will use functions from [34] to get upper and lower error bands, i.e. we will count jet with upper/lower weights to calculate uncertainty.

In Table 24 we summarize number of events in the electron-photon and muon-photon samples for various categories analyzed.

4.6.2 Electron Faking Photon

In Table 25 we summarize numbers of events in electron-photon sample and Zee sample for various categories analyzed.

Using numbers from Table 25 we calculate background from electrons misidentified as photons. For a given subcategory the estimated number of electron-fake-photon events("Fakes") will be calculated as follows:

$$N_{subcategory}^{\mathrm{Z}^0 \rightarrow e^+e^-} * \frac{N_{Z^0 0-like}^{e\gamma} - N_{Z^0 0-like}^{diboson} - N_{Z^0 0-like}^{jets}}{N_{Z^0 0-like}^{\mathrm{Z}^0 \rightarrow e^+e^-}} \quad (2)$$

where

- $N_{subcategory}^{\mathrm{Z}^0 \rightarrow e^+e^-}$ - number of events in $\mathrm{Z}^0 \rightarrow e^+e^-$ sample for a given subcategory

Categories	All Other	1 l, 1 γ, $\Delta\phi$ <150	$\ell\gamma \not\!\!E_T$	Multi-Lepton	Multi-Photon
Electron	2.18 ± .76	1.16 ± .41	.90 ± .32	.12 ± .04	.00009 ± .00003
Muon	.49 ± .17	.07 ± .02	.36 ± .13	.05 ± .02	.00001 ± 0
Lepton	2.67 ± .77	1.23 ± .41	1.26 ± .34	.17 ± .04	.00010 ± .00003

Table 24: Jet Faking Photon: predicted backgrounds in different subcategories. We take error on the predicted number to be 35%

Categories	Z^0-like	All Other	1 l, 1 γ, $\Delta\phi$ <150	$\ell\gamma \not\!\!E_T$	Multi-Lepton	Multi-Photon
$Z^0 \to e^+e^-$	3172	357	314	36	7	2
Diboson	5.70 ± .23	24.49 ± .75	5.00 ± .24	9.48 ± .63	9.32 ± .27	.02648 ± .0114648
Jet Fakes	1.47 ± .52	2.18 ± .76	1.16 ± .41	.90 ± .32	.12 ± .04	.00009 ± .00003
Fakes	89.83 ± 9.86	10.11 ± 1.11	8.89 ± .98	1.02 ± .11	.20 ± .02	.057 ± .006

Table 25: Electron Faking Photon: number of events in different subcategories

- $N^{e\gamma}_{Z^0 0-like}$ - number of $Z^0 - like$ events in electron-photon sample
- $N^{diboson}_{Z^0 0-like}$ - number of $Z^0 - like$ events expected from diboson events
- $N^{jets}_{Z^0 0-like}$ - number of $Z^0 - like$ events expected from misidentified jets
- $N^{\mathrm{Z}^0 \to e^+e^-}_{Z^0 0-like}$ - number of "$Z^0 - like$" events in $\mathrm{Z}^0 \to e^+e^-$ sample(81 GeV < M^0_Z < 101 GeV), $\Delta\phi > 150$))

We require both electron in $\mathrm{Z}^0 \to e^+e^-$ to be central and pass tight cuts, so that the kinematic requirements will be the same as for the photon-electron sample(two tight central electromagnetic objects).

For example, to estimate electron-fake-photon events in $\ell\gamma \not\!\!E_T$ photon-electron events

$$36 * \frac{97 \pm 9.84 - 5.70 \pm .23 - 1.47 \pm .52}{3172} = 1.02 \pm .11 \quad (3)$$

5 Photon-Lepton Events

In order to compare directly with the previous Run I analysis [11], we use the same categories for event classification [36], as shown in Figures 19 and 20. The lepton-photon sample requires only a tight lepton and a tight photon with $E_T > 25$ GeV, plus anything else. From this sample we select back-to-back events with exactly one photon and one lepton; this is the dominant contribution to the lepton-photon sample, and has a large Drell-Yan component. A subset of this sample is the 'Z-like' sample, for which the photon and the lepton have an invariant mass within 10 GeV of the Z^0 mass; this sample provides the calibration for the probability that an electron radiates and is detected as a photon, as discussed in Section 3.6.3. The remaining back-to-back events are called the Two-Body Events, and are not used in this analysis.

All events which either have more than one lepton or photon, or in which the lepton and photon are not back-to-back, are classified as 'Inclusive Multi-Body Events'. These are further subdivided into three categories: 'Multi-Body $\ell\gamma\not{E}_T$ Events', for which the $\not{E}_T$ is greater than 25 GeV, 'Multi-Photon and Multi-Lepton Events', and events with exactly one lepton and exactly one photon, which are not back-to-back [36], Figure 18.

Figure 19 shows the results of this classification to the inclusive electron data sample. We find 249 electron-photon events, of which 45 are in the Inclusive Multi-Body category. Of these, 8 are classified as $\ell\gamma\not{E}_T$ events and 0 and 7 as Multi-Photon and Multi-Lepton events respectively.

Figure 20 shows the results for the inclusive muon sample.We find 27 muon-photon events, of which 15 are in the Inclusive Multi-Body category. Of these, 6 are classified as $\ell\gamma\not{E}_T$ events and 0 and 6 as Multi-Photon and Multi-Lepton events. It is these last two categories that are of particular interest due to the Run I results.

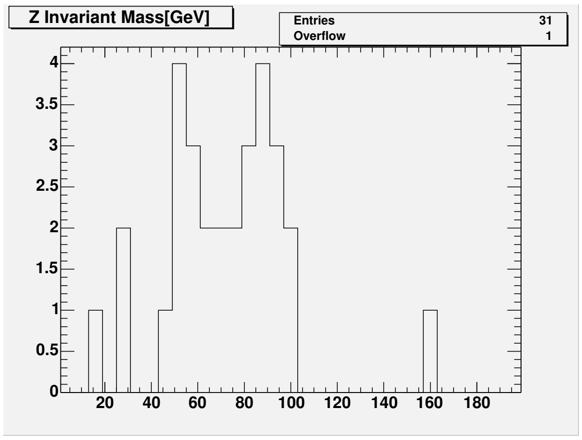

(a) Invariant Mass

Figure 18: Distribution of Invariant Mass of $Z \to e`\gamma`$ for events with exactly one lepton and exactly one photon, but not back-to-back [36]. We don't require CENTRAL_ELECTRON_18 trigger.

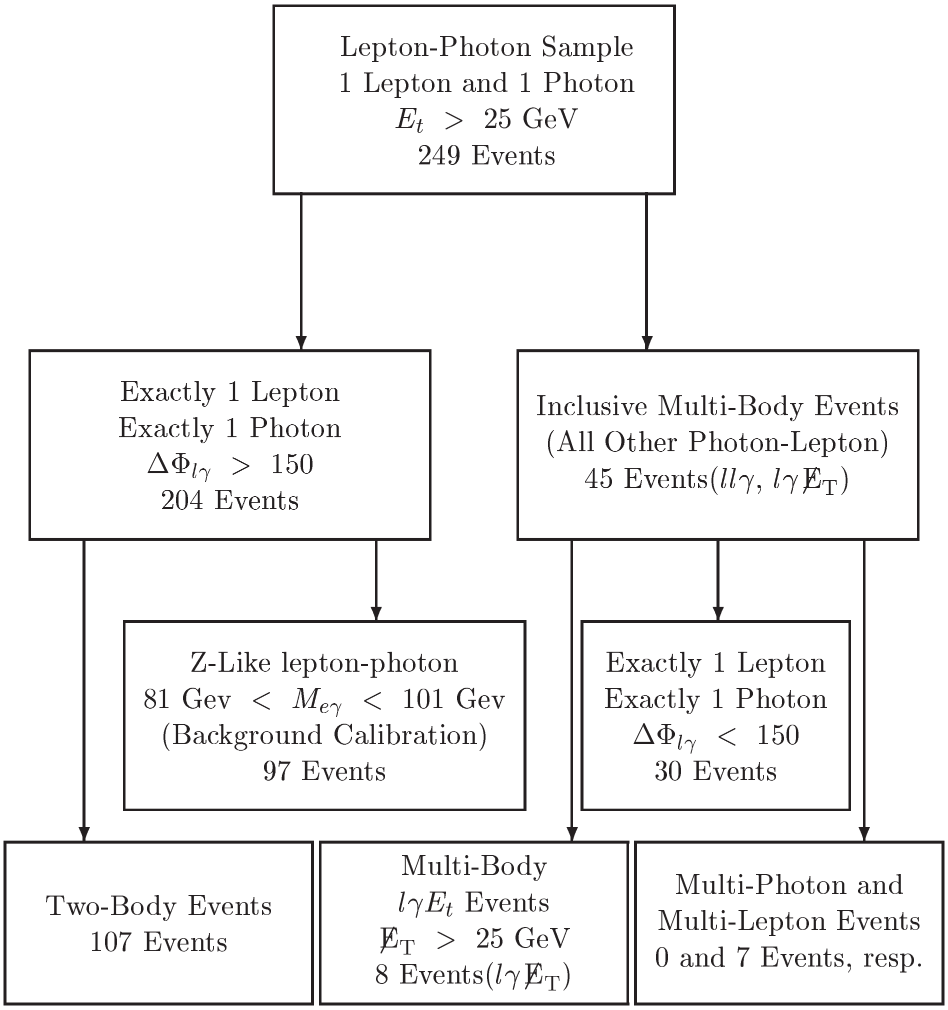

Figure 19: Photon-Electron Sample: the subsets of inclusive γl events analyzed in this paper

6 Conclusions

The Run I search was initiated by an anomaly in the data itself ; however, we set cuts *a priori* to calculate the statistical probability of getting a specific result. So initially we have set the Run II selection criteria to be the same as for Run I, so as to make a direct repeat but with substantially more data.

We find 14 $\ell\gamma\not{E}_T$ events (8 in the $e\gamma$ channel and 6 in the $\mu\gamma$ channel) versus a Standard Model expectation of $18.81 \pm .95$ ($11.46 \pm .70$ and $7.37 \pm .64$) events. There are 13 (7 and 6) multilepton+gamma and 0 (0 and 0) multigamma+lepton events, versus expectations of $14.38 \pm .33$ ($9.46 \pm .27$ and $4.94 \pm .19$) and $.02040 \pm .0049043$ ($.01664 \pm .0045196$ and $.00480 \pm .0019040$) events, respectively.

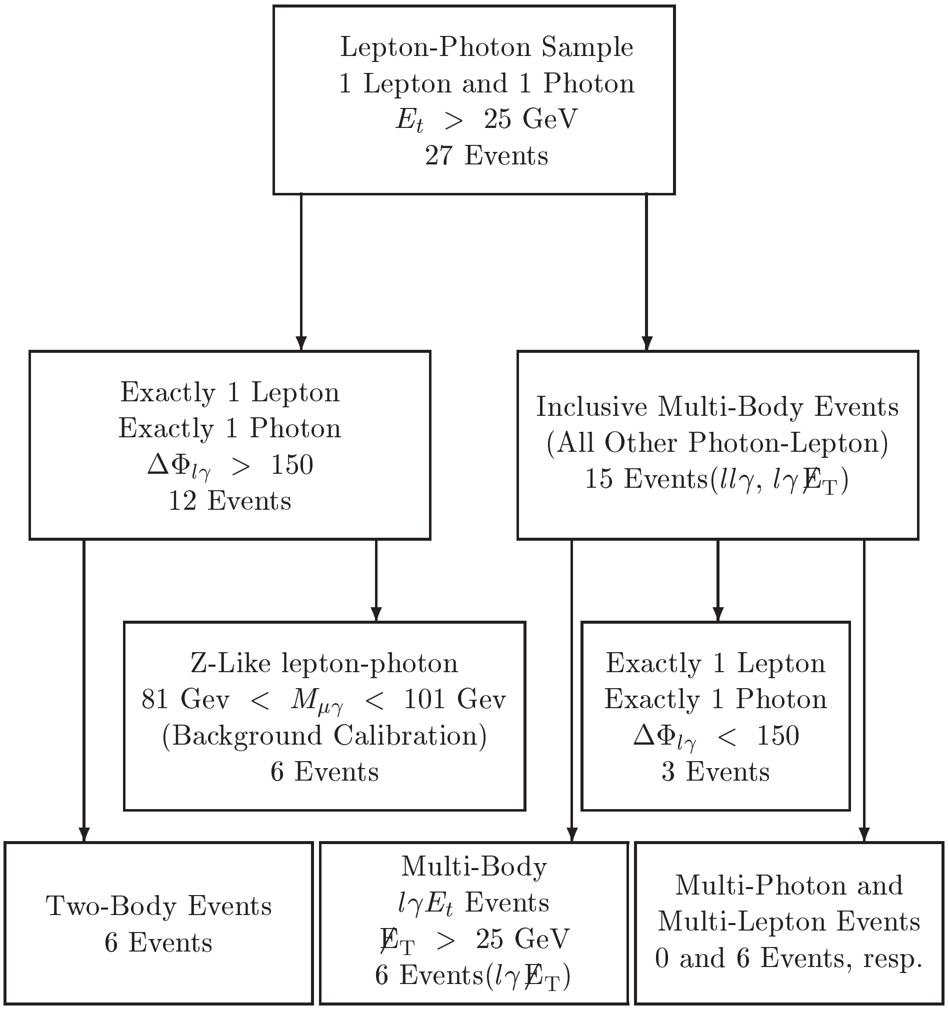

Figure 20: Photon-Muon Sample: the subsets of inclusive γl events analyzed in this paper

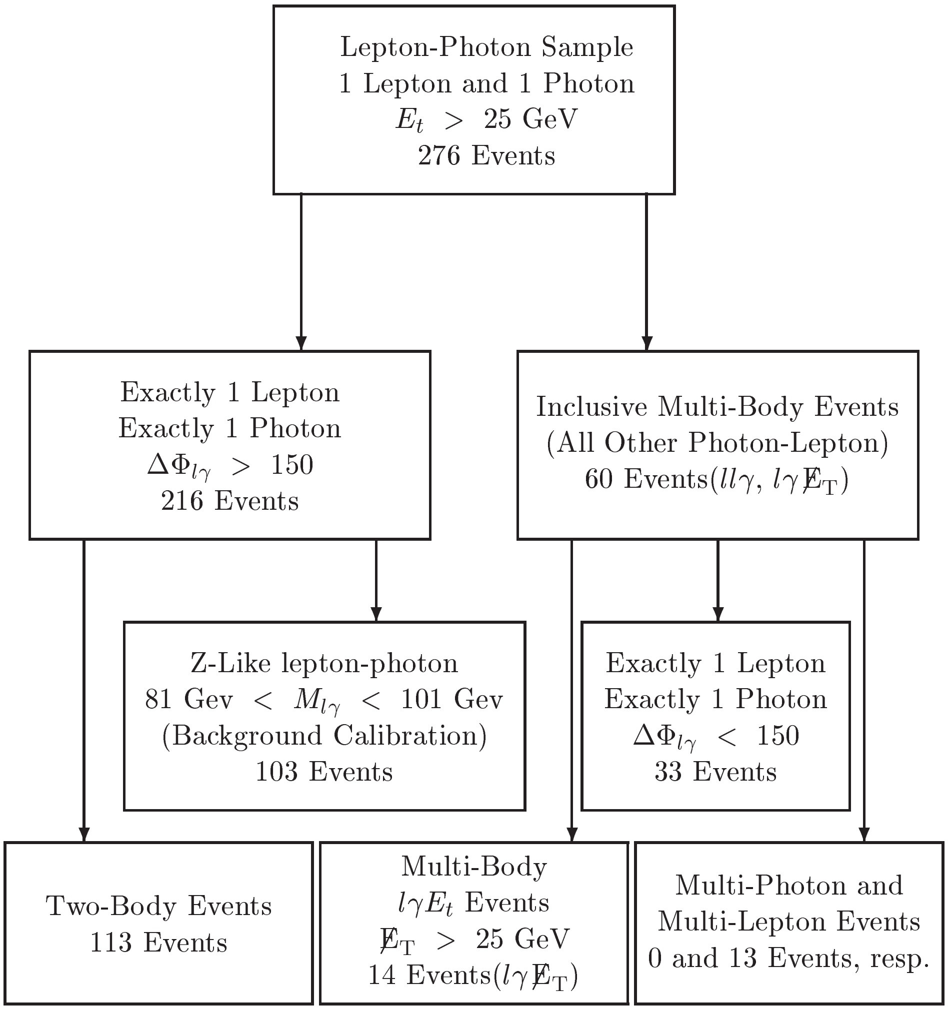

Figure 21: Photon-Lepton Sample: the subsets of inclusive γl events analyzed in this paper

Lepton+ Gamma $+\not\!\!E_T$ Predicted Events: 200 pb^{-1}			
Standard Model Source	$e\gamma\not\!\!E_T$	$\mu\gamma\not\!\!E_T$	$(e+\mu)\gamma\not\!\!E_T$
$W^{\pm}\gamma$	8.39 ± 0.631	4.01 ± 0.435	$12.40 \pm .76$
$Z^0\gamma$	1.03 ± 0.0919	2.01 ± 0.129	$3.04 \pm .15$
$W^{\pm}\gamma\gamma$	0.0476 ± 0.00289	0.0322 ± 0.00238	$.07980 \pm .0037438$
$Z^0\gamma\gamma$	0.02 ± 0.00427	0.0654 ± 0.00771	$.08540 \pm .0088134$
$Z^0 \to e^+e^-, e \to \gamma$	$1.02 \pm .11$	-	$1.02 \pm .11$
Jet faking γ	$.90 \pm .32$	$.36 \pm .13$	$1.26 \pm .34$
Hadron faking e, μ $+\gamma$(*)	-	0.54 ± 0.33	0.54 ± 0.33
π/K Decay-in-Flight $+\gamma$(*)	-	0.30 ± 0.33	0.30 ± 0.33
Heavy Flavor Decay $+\gamma$(*)	$< .03$	$< .03$	< 0.06
Total SM Prediction	$11.46 \pm .70$	$7.37 \pm .64$	$18.81 \pm .95$
Observed in Data	8	6	14

Table 26: The predicted number of lepton-photon-$\not\!\!E_T$ events in 200 pb^{-1} from Standard Model sources, and the numbers of events observed. The $W\gamma$ and $Z\gamma$ numbers are the weighted averages of MadGraph, CompHep, and Baur predictions, multiplied by a K-factor of 1.36. The $W\gamma\gamma$ number is the average of MadGraph and CompHep, while the $Z\gamma\gamma$ is MadGraph alone (the CompHep sample has cuts that are too restrictive). Both the $W\gamma\gamma$ and $W\gamma\gamma$ predictions have also been multiplied by the same K-factor. (*) These numbers are scaled Run I numbers

Multi-Lepton +Gamma + X Predicted Events: 200 pb^{-1}			
Standard Model Source	$ee\gamma + X$	$\mu\mu\gamma + X$	$ll\gamma + X$
$Z^0\gamma$	9.12 ± 0.274	4.82 ± 0.199	$13.94 \pm .33$
$Z^0\gamma\gamma$	0.184 ± 0.0129	0.0518 ± 0.00687	$.23 \pm .0146152$
Z^0+Jet, jet faking γ	$.12 \pm .04$	$.05 \pm .02$	$.17 \pm .04$
Total SM Prediction	$9.46 \pm .27$	$4.94 \pm .19$	$14.38 \pm .33$
Observed in Data	7	6	13

Table 27: The predicted number of multi-body events with additional leptons in 200 pb^{-1} from Standard Model sources, and the numbers of events observed. The $Z\gamma\gamma$ prediction is from MadGraph alone (the CompHep sample has cuts that are too restrictive). The Z^0+Jet and $W\gamma$+Jet predictions are taken from the data; the MC predictions have also been multiplied by the same K-factor (see text).

Multi-Gamma +Lepton + X Predicted Events: 200 pb^{-1}			
Standard Model Source	$e\gamma\gamma + X$	$\mu\gamma\gamma + X$	$l\gamma\gamma + X$
$W^{\pm}\gamma\gamma$	0.00258 ± 0.000676	0.00169 ± 0.000545	$.00427 \pm .0008683$
$Z^0\gamma\gamma$	0.0109 ± 0.00316	0.00182 ± 0.00129	$.01272 \pm .0034131$
Total SM Prediction	$.01664 \pm .0045196$	$.00480 \pm .0019040$	$.02040 \pm .0049043$
Observed in Data	0	0	0

Table 28: The predicted number of multi-body events with additional leptons in 200 pb^{-1} from Standard Model sources, and the numbers of events observed. The $Z\gamma\gamma$ prediction is from MadGraph alone (the CompHep sample has cuts that are too restrictive). the MC predictions have also been multiplied by the same K-factor (see text).

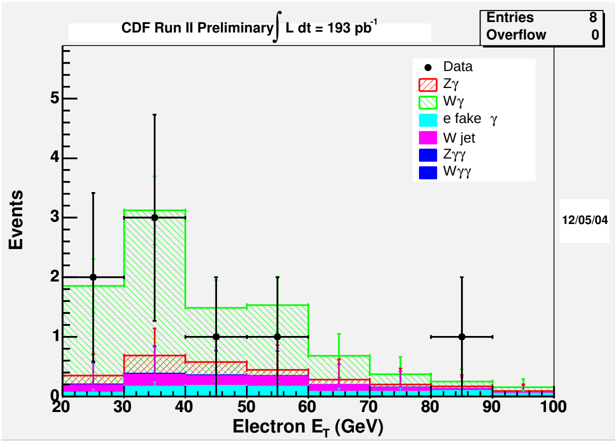

(a) Electron P_T

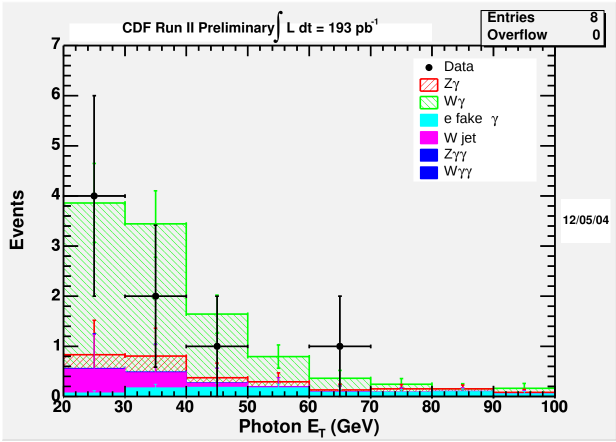

(b) Photon P_T

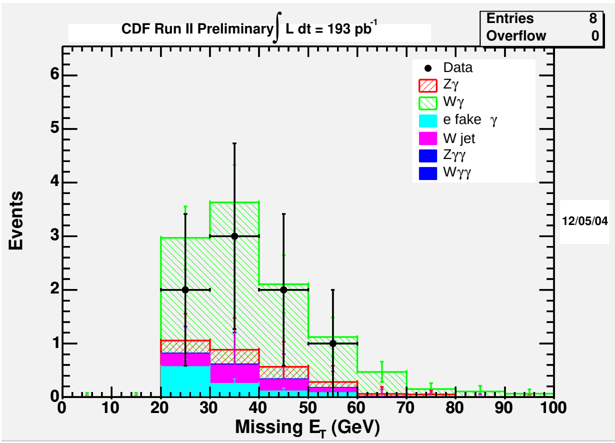

(c) $\not\!\!E_T$

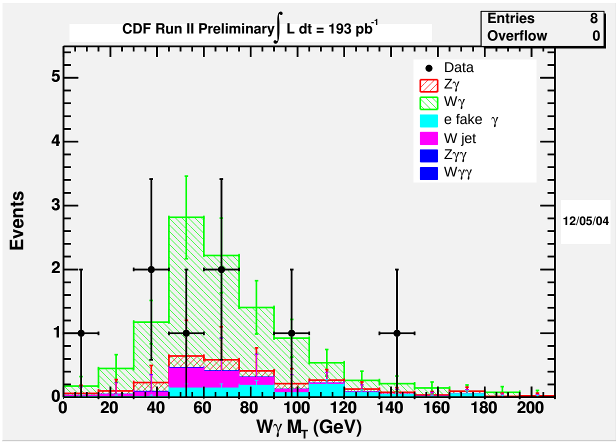

(d) $Z^0\gamma$ Invariant Mass

Figure 22: Lepton-Gamma-Met Distributions: Electron Channel

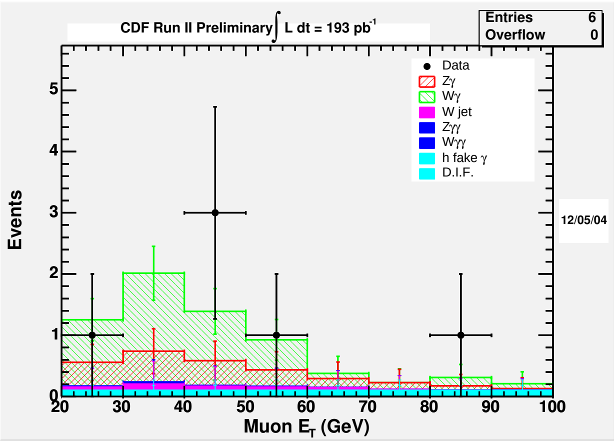

(a) Muon P_T

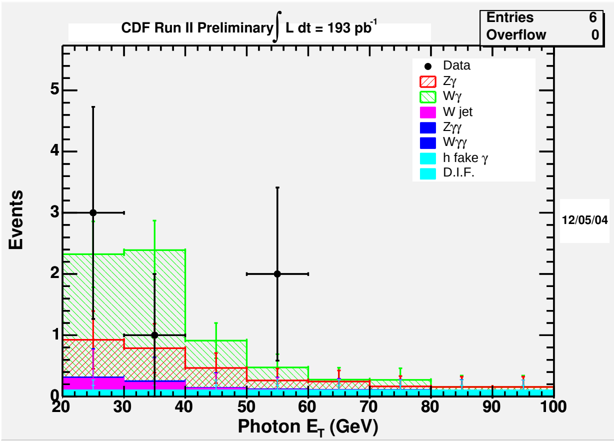

(b) Photon P_T

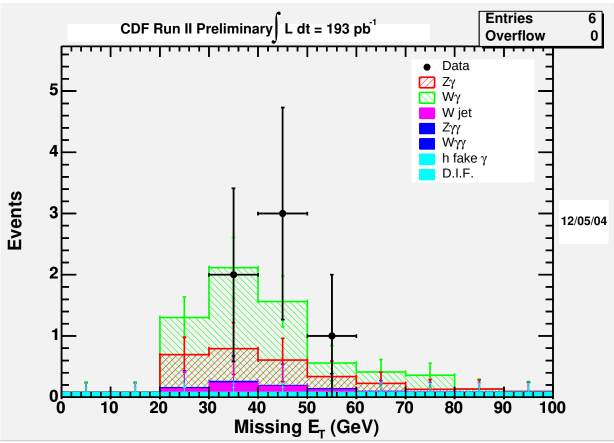

(c) $\not{E}_T$

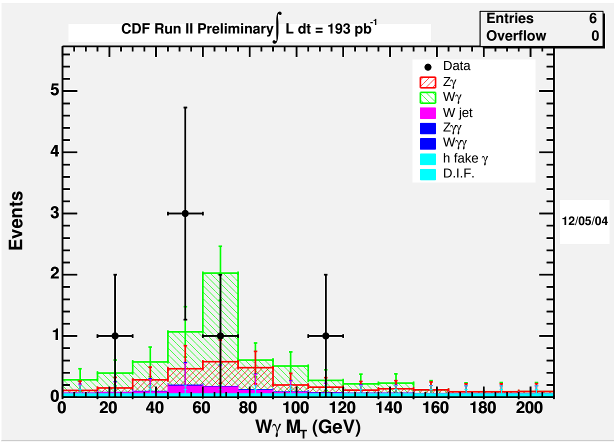

(d) $Z^0\gamma$ Invariant Mass

Figure 23: Lepton-Gamma-Met Distributions: Muon Channel

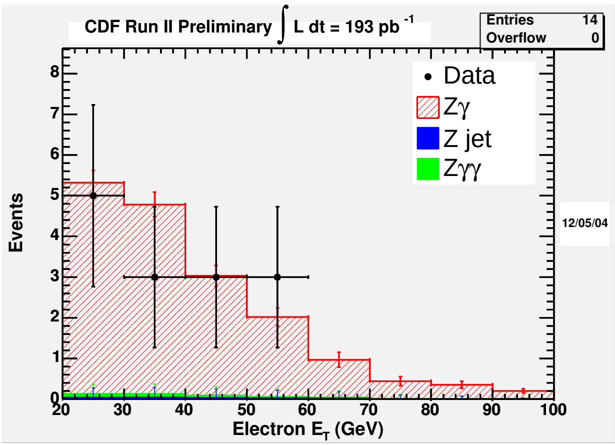

(a) Electron P_T

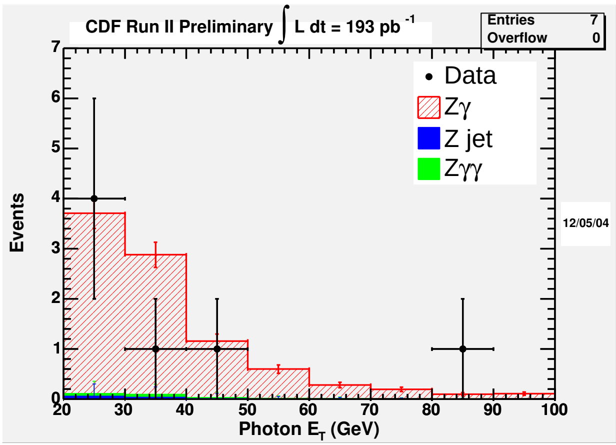

(b) Photon P_T

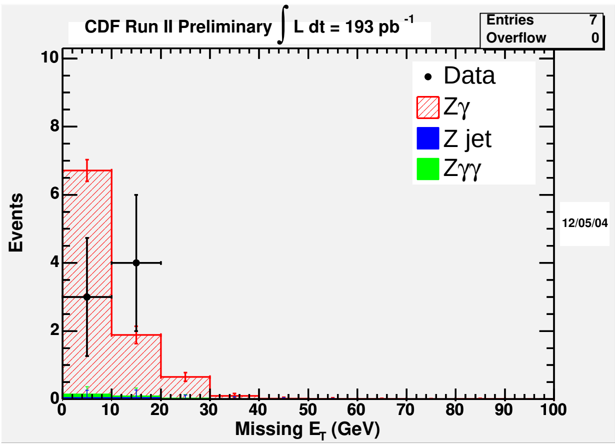

(c) $\not{E}_T$

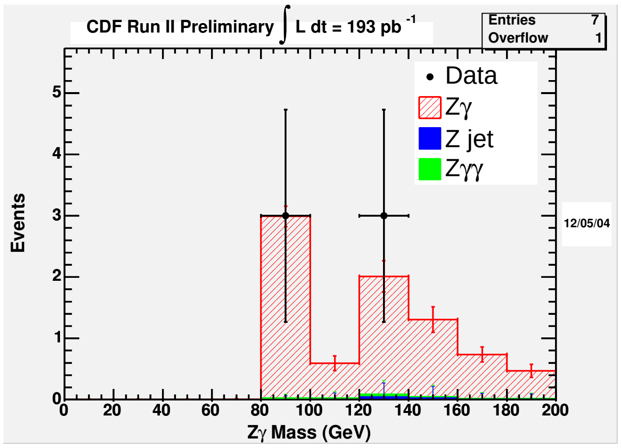

(d) $Z^0\gamma$ Invariant Mass

Figure 24: Multi-Lepton-Gamma Distributions: Electron Channel. Overfloat: run/event 154518/1101736, Mass($Z\gamma$) = 268.584, $P_T(Z\gamma)$ = 10.1884

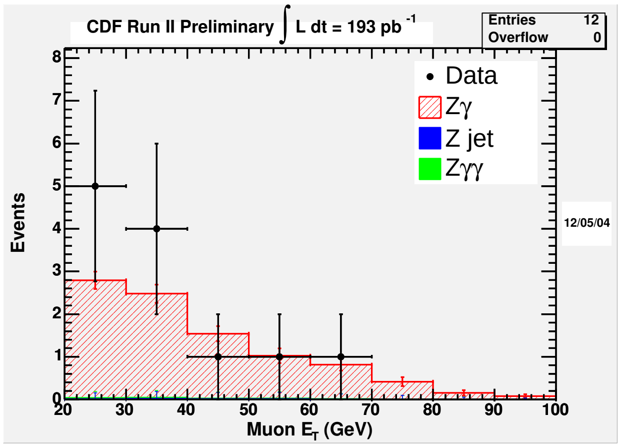

(a) Muon P_T

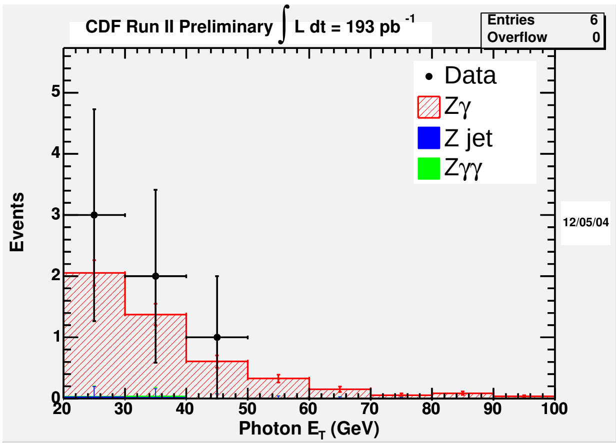

(b) Photon P_T

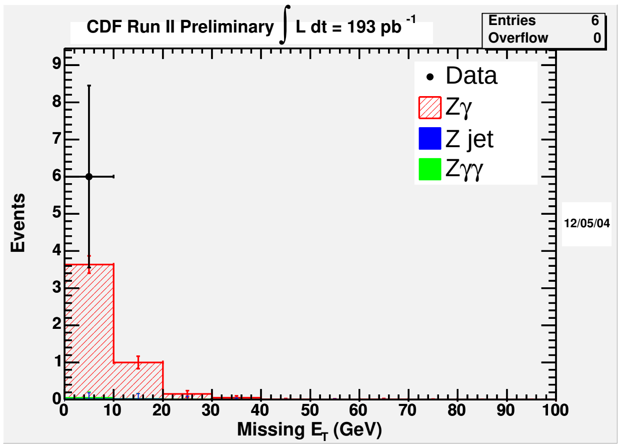

(c) $\not\!\!E_T$

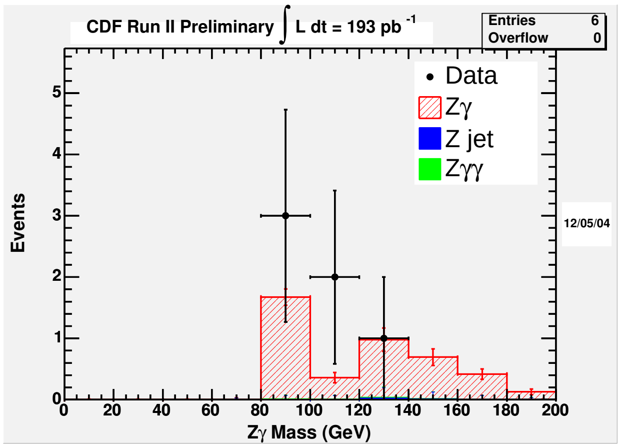

(d) $Z^0\gamma$ Invariant Mass

Figure 25: Multi-Lepton-Gamma Distributions: Muon Channel

7 Acknowledgements

We thank Andrei Rostovtsev for his encouragement and support. We also owe thanks to Eduard Boos and Lev Dudko for their support and development of CompHep, and Tim Steltzer, Steve Mrenna, and Fabio Maltoni for their similar responsiveness for MadGraph and Pythia. Alexander Belyaev, and Alexander Sherstnev generated the CompHep $W\gamma\gamma$ and $Z\gamma\gamma$ datasets, respectively, for us. Uli Baur provided wisdom on the effective Born approximation parameters for the LO parameters. We also would like to thank our CDF collaborators Ray Culbertson, Beate Heinemann, Mike Kirby, Steve Levy, Reda Tafirout, Stan Thompson, Jason Tsui, Soushi Tsuno, and Un-Ki Yang for their many contributions.

8 Appendices

8.1 Appendix A: List of good runs

8.2 Appendix B: List Of Lepton-Photon Events

8.2.1 Electron-Photon Events

	γ			ℓ					$\ell\gamma$		$\not\!\!E_T$	
run/event	pt	phi	eta	type	pt	phi	eta	trg	dphi	InvM	$\not\!\!E_T$	phi
152520/1501463	31	-0.69	-0.27	CEM	28	1.7	0.14	1	2.4	56	11	3
152520/2763531	42	-1.7	0.66	CEM	43	1.5	0.058	1	3.1	89	6.9	6
152554/833369	47	2.9	-0.7	CEM	45	-0.17	-0.19	1	3	95	3.1	5.1
152600/247769	88	-0.6	0.78	CEM	45	2.1	0.63	1	2.7	1.2e+02	21	2.6
145654/3433141	28	0.76	0.77	CEM	29	-2.5	0.9	1	3	57	5.2	4.3
152809/40469	33	1.1	0.47	CEM	27	-1.9	0.74	1	3.1	60	5.6	4
152810/999944	41	0.62	0.39	CEM	47	-2.5	-0.066	1	3.1	91	2	2.2
152954/362678	34	2.2	0.77	CEM	43	-0.69	-0.59	1	2.9	95	5.6	4.3
153074/1339595	26	-0.33	-0.18	CEM	40	-1.3	-0.99	1	1	40	27	0.47
153327/4778229	33	1.1	-0.59	CEM	47	-2.5	0.73	1	2.7	96	4.3	5.3
153372/392004	46	-2.7	-0.99	CEM	42	0.5	-0.31	1	3.1	92	5.2	6.3
153389/6622875	28	2.1	0.8	CEM	45	-0.96	-0.61	1	3.1	90	7.8	2.2
153416/2387528	26	2.3	-0.094	CEM	34	-0.67	-0.7	1	3	63	9.1	2.9
153447/3341967	27	-1.9	1	CEM	29	2.2	-0.99	1	2.2	82	0.6	0.31
153447/3690142	26	1.3	0.41	CEM	26	-1.7	0.62	1	3	52	4.3	4.6
153662/723772	25	0.94	-0.9	CEM	32	1.2	0.59	0	0.21	45	54	4.1
153693/1425631	33	1.2	0.4	CEM	34	-1.8	0.12	1	3	67	7.2	3.4
153718/139182	26	-0.74	0.85	CEM	34	2.2	-0.97	1	2.9	86	1.3	5.1
153718/1168201	32	1.5	0.6	CEM	27	-1.7	0.17	1	3	60	2.5	5.5
153718/1401721	39	-0.38	0.073	CEM	45	-2.8	-0.59	1	2.4	83	13	1
153738/2261542	93	-2.8	0.34	CEM	85	0.4	0.71	1	3.1	1.8e+02	13	5.9
154021/2044250	31	1.2	-0.069	CEM	38	-1.3	-0.13	1	2.6	66	1.5	3.3
154070/2326729	28	-1.3	0.98	CEM	26	1.7	0.35	1	3.1	57	1.5	2.7
154070/1683413	48	-2.1	0.6	CEM	45	0.48	0.52	1	2.5	88	6.6	3
154070/2190018	25	1.2	-0.65	CEM	32	-0.9	-0.84	1	2.1	50	8.6	2.5
154111/1220755	33	0.65	-0.12	CEM	31	-2.4	-0.34	1	3	65	5.5	2
154111/1838920	28	0.72	-0.51	CEM	25	-2.2	0.62	1	2.9	61	3.4	1.8
154126/1748439	37	-2.4	0.44	CEM	43	0.87	-0.38	0	3	87	12	4.4
154175/528261	25	1	0.89	CEM	27	-2.2	-0.51	1	3.1	66	1.2	2.9
154175/1903834	32	-2.3	0.58	CEM	39	0.71	0.36	1	3	72	11	4.7
154180/131287	29	3	0.42	CEM	32	-0.5	-0.97	1	2.7	74	8.4	4.1
154180/1693139	32	-2.7	0.57	CEM	27	0.37	-0.34	1	3.1	65	4.2	0.66
154208/434924	45	0.57	-0.38	CEM	41	-2.8	0.43	1	2.9	93	10	4
154452/3786468	31	2.6	-0.48	CEM	27	-0.94	0.21	1	2.8	60	16	5.2
154452/4063974	27	1.5	-0.67	CEM	29	-1.5	-0.54	1	3	56	4.8	1.9
154518/137940	64	-1.5	-0.67	CEM	50	1.5	-0.75	1	3.1	1.1e+02	20	1.3
154518/475545	44	-1.5	0.5	CEM	43	1.5	-0.24	1	3	92	2.4	1.3
154518/1101736	83	-1.5	-0.14	CEM	48	1.4	-0.72	1	2.9	1.3e+02	1.9	6.3
				EPLUG	46	1.9	-2.4	1	2.8	2.2e+02		
154653/124572	50	-2.5	0.13	CEM	41	0.68	-0.27	1	3.1	93	8.7	0.34
154654/1407470	41	1.7	-0.37	CEM	43	-1.3	0.75	1	3	99	10	4.8

Continued on next page

Table 29 – continued from previous page

154654/2794426	45	1.9	-0.89	CEM	43	-1.2	-0.23	1	3.1	93	6.3	2.1
154654/5753858	33	2.7	0.19	CEM	43	-0.48	0.79	1	3.1	78	2.1	3.1
154768/579038	46	-2.5	0.46	CEM	47	0.58	0.93	1	3	95	7	4.6
154768/2109541	43	-0.58	0.73	CEM	37	2.7	-0.37	1	3	92	6.8	1.3
154768/4316113	25	0.88	-0.96	CEM	32	-2.3	-0.88	1	3.1	56	2.9	5.6
148291/463689	33	-0.62	-0.31	CEM	31	2.7	-0.48	1	3	64	0.081	3.7
155113/2299668	38	-2.8	0.58	CEM	38	0.36	-0.53	1	3.1	87	4.4	5.7
155130/669237	39	2.2	1	CEM	50	-0.5	0.38	1	2.7	93	3.6	3.3
155130/3896752	45	2.5	0.68	CEM	37	-0.48	0.16	1	3	85	1.9	2.2
155345/3484741	35	0.39	0.76	CEM	39	-2.4	-0.49	1	2.8	88	3.2	3.3
155364/3510152	34	-2.9	0.61	CEM	29	0.69	-0.12	1	2.7	66	18	5.2
148674/560257	42	-3.1	0.71	CEM	38	0.034	-0.51	1	3.1	95	0.52	4.1
155743/721912	37	1.2	-0.32	CEM	69	-2	0.49	1	3.1	1.1e+02	6	1.4
155746/2061472	37	2.9	0.97	CEM	42	-0.31	0.59	1	3	80	10	3.9
155770/2888444	42	-3	0.88	CEM	47	0.12	0.97	1	3.1	89	4.5	5.3
155795/1471034	31	0.19	0.69	CEM	36	-3.1	0.16	1	3	69	4.3	5.8
155795/4487113	25	-0.85	-0.41	CEM	50	2.4	0.79	1	3	83	19	5.3
156007/1423050	35	-2.7	0.47	CEM	45	0.15	0.81	1	2.8	80	7	2.9
156081/1296589	54	0.42	0.22	CEM	61	-2.8	-0.98	1	3.1	1.3e+02	7	1.1
156083/1091219	35	2.1	-0.19	CEM	33	1.1	0.37	1	1.1	40	60	4.7
156089/1764179	35	2.3	0.64	CEM	41	-0.89	0.1	1	3.1	78	9.5	2.8
156116/2094822	40	-1.5	0.28	CEM	43	1.7	-0.57	1	3.1	91	3.7	5.3
156484/119387	31	-1.9	0.64	CEM	36	1.7	-0.19	1	2.7	71	7.6	5.5
156484/2846125	60	0.48	0.96	CEM	38	-2.8	1	1	3	95	11	3.6
160823/1189235	40	-1.6	0.56	CEM	39	1.5	-0.38	1	3.1	88	5.4	1.3
160823/2337658	51	1.7	-0.97	CEM	55	-1.5	-0.4	1	3.1	1.1e+02	4.3	0.45
160890/2049483	72	2.8	-0.89	CEM	73	0.72	0.36	1	2	1.6e+02	22	4.6
160891/2869094	32	-2.4	0.41	CEM	36	1.2	0.28	1	2.7	66	6.4	4.3
160891/3399714	33	1.7	0.15	CEM	43	0.62	-0.38	1	1.1	45	12	4.9
148856/197868	44	-0.2	-0.31	CEM	44	3	-0.72	1	3.1	90	1.3	1.1
161011/1768764	62	-3.1	-0.79	CEM	56	0.22	-0.86	1	2.9	1.2e+02	11	5.3
161011/3897893	30	-1.1	0.96	CEM	29	2	0.54	1	3.1	60	2.1	3.7
161029/257314	58	-2.5	0.59	CEM	36	0.82	-0.33	1	3	1e+02	21	0.62
161324/58271	47	-1.2	0.71	CEM	48	2	0.67	1	3.1	95	1.1	3.6
161330/149228	38	0.17	-0.26	CEM	26	-3.1	-0.41	1	3.1	63	11	3
161330/3735878	44	-2	-0.35	CEM	38	1	-0.63	1	3.1	83	1.7	1.5
161379/494836	93	-0.16	0.75	CEM	1.5e+02	2.1	0.19	1	2.3	2.2e+02	16	4.9
161379/6291037	26	-0.073	0.088	CEM	32	2.8	-0.73	1	2.9	63	7.5	2.6
161411/549376	42	1.9	0.82	CEM	49	-1.4	1	1	3	90	9.8	1.1
161552/80426	27	-0.6	-0.12	CEM	31	2.5	-0.6	1	3.1	60	9.3	5.5
161552/1272218	28	0.66	-0.73	CEM	43	-2.2	0.85	1	2.8	91	9.9	3.7
161552/3322465	45	0.4	-0.39	CEM	37	-2.7	0.68	1	3.1	95	8.2	5.5
161552/4609663	42	-1.6	0.58	CEM	47	0.73	-0.65	1	2.4	1e+02	21	3.7
161633/1832555	37	-0.32	0.36	CEM	41	-2.4	-0.74	1	2.1	80	14	0.77
161633/2528326	27	2.1	-0.42	CEM	32	-1.4	-0.92	1	2.7	59	1.3	6.2
161633/2624127	39	-1.4	0.69	CEM	44	1.9	-0.25	1	3	92	6.1	5.4
148916/384086	25	1	0.06	CEM	43	-1.7	-0.45	1	2.8	67	1	6
148950/505683	25	1.6	-0.89	CEM	26	-1.6	-0.73	1	3	52	2.4	1.5
161633/4895788	44	0.12	-0.27	CEM	42	-3	0.19	1	3.1	88	7.2	0.65
161678/2386632	27	-0.46	-0.58	CEM	45	2.6	-0.75	1	3.1	69	3	5.3

Continued on next page

Table 29 – continued from previous page

161678/7976298	34	2.9	-0.42	CEM	40	0.13	0.87	1	2.8	89	4.9	5.1
161714/1613952	45	2.8	0.088	CEM	43	-0.39	0.062	1	3.1	88	3.3	5.6
161786/335331	27	2.2	-0.91	CEM	49	-0.49	-0.073	1	2.7	77	23	2.9
161829/23487	55	1.1	-0.42	CEM	38	-2	-0.48	1	3.1	92	8.6	4.1
162130/1818679	35	-1.1	0.16	CEM	36	1.8	0.92	1	2.9	75	6	1.2
162130/3258766	32	-0.93	-0.47	CEM	37	2.4	-0.31	1	2.9	69	6.4	5.3
162175/1384238	31	1.5	-0.62	CEM	32	-1.7	0.59	1	3.1	75	2.5	6.2
162178/1231337	43	2.5	-0.87	CEM	49	-0.48	-0.99	1	2.9	91	7.8	4.4
162178/2188093	45	-1.1	0.69	CEM	48	2	-0.99	1	3.1	1.3e+02	3.1	2.3
162178/4214317	37	-2.2	-0.22	CEM	34	1	-0.31	1	3.1	71	7.8	0.36
162241/760631	44	-0.34	-0.49	CEM	44	2.8	-0.082	1	3.1	89	3.7	4.4
162307/444051	45	-2.5	0.25	CEM	45	0.61	0.79	1	3.1	92	3	5.9
162310/1505729	35	-0.9	-0.31	CEM	44	-0.9	0.44	1	0.006	29	14	2.2
149059/603455	45	-2.6	-0.63	CEM	42	0.7	-0.86	1	3	87	1.6	5.4
162396/1323030	27	0.55	-0.99	CEM	42	-2.8	-0.95	1	2.9	66	5.4	0.75
				CEM	21	0.15	-0.39	1	0.4	16		
162423/690231	62	2.5	-0.64	CEM	89	-0.63	0.58	1	3.1	1.8e+02	1.9	1.5
149344/204664	41	0.23	0.27	CEM	43	-3.1	0.83	1	3	87	7	5.2
149386/1425067	26	-0.17	-0.069	CEM	33	0.048	0.43	1	0.22	16	5.4	3.1
162480/3707495	38	-0.34	0.35	CEM	29	2.7	-0.46	1	3	71	6.7	2.5
162480/3928304	37	1.9	-0.25	CEM	31	-1.4	-0.36	1	2.9	67	6.5	5.5
144713/2420258	40	1.3	1	CEM	39	-1.9	0.57	1	3.1	81	3.6	5.6
149387/1099516	30	3.1	-0.36	CEM	57	-0.42	-0.38	1	2.7	80	10	5
				CEM	31	2.4	0.45	1	0.7	33		
149387/2185350	35	2.2	-0.19	CEM	32	-1.2	-0.49	1	2.9	67	13	6
159610/782350	43	-1.8	-0.14	CEM	45	1.4	-0.43	1	3.1	89	5.4	6.2
160152/687378	52	-1.2	0.92	CEM	34	2	0.62	1	3	85	11	1.7
160152/769331	43	2.9	0.66	CEM	46	-0.36	0.36	1	3	90	4.8	1.2
160175/41637	34	2.8	-0.95	CEM	36	-0.44	-0.92	1	3	70	6.4	2
160175/2435369	28	1.8	0.13	CEM	25	-1.5	0.45	1	3	54	2.9	0.26
160229/212201	49	0.65	-0.2	CEM	34	-2.6	-0.64	1	3	83	6.5	3.7
160230/100945	47	-0.54	0.6	CEM	48	2.6	0.64	1	3.1	95	2.3	0.77
160314/357265	28	0.97	-1	CEM	57	-2.4	0.3	1	2.9	99	7.5	0.15
160346/1182158	45	2	-0.87	CEM	45	-1.2	-0.38	0	3.1	92	7.1	4.8
160346/1528176	46	-0.82	-0.87	CEM	50	-3.1	-1	1	2.3	88	16	1.4
				CEM	25	0.81	-0.94	1	1.6	49		
160441/1280211	30	1.7	-0.66	CEM	32	-0.91	0.65	1	2.6	74	13	2.3
160441/1316398	29	-1.4	0.17	CEM	31	1.7	-0.71	1	3.1	65	5.6	1.5
149678/19819	26	3.1	0.21	CEM	28	-0.23	-0.52	1	3	57	4.8	0.91
160591/46155	29	2	0.84	CEM	41	-1.1	0.31	1	3.1	71	2.1	5.7
160593/304908	38	0.95	-0.22	CEM	44	-2.3	0.61	1	3.1	90	5.9	0.58
160600/152621	27	-2.1	0.33	CEM	27	1.1	0.99	1	3	57	5	6.1
160663/1812389	27	-0.58	0.38	CEM	50	2.6	0.52	1	3.1	74	1.2	4.6
160796/3129783	38	-2.2	-0.26	CEM	46	1	-0.91	1	3	88	8.3	4.4
149685/156214	42	0.16	0.28	CEM	45	-3	-0.17	0	3.1	90	7.6	0.94
162480/6015084	42	-0.064	0.57	CEM	47	3	0.81	1	3.1	89	6	5.8
162498/573907	76	2.3	-0.85	CEM	79	-0.91	-1	1	3.1	1.5e+02	2	2.3
162664/3203602	48	1.7	-0.54	CEM	42	-1.5	-0.76	1	3.1	90	8.1	5
162664/4829187	28	-1.2	-0.66	CEM	45	2.4	-0.46	1	2.7	70	18	6.2
162836/996381	62	2.8	0.41	CEM	59	-0.72	0.22	1	2.8	1.2e+02	25	6.1

Continued on next page

Table 29 – continued from previous page

162837/1400343	41	-1	0.15	CEM	38	2.2	-0.32	1	3.1	81	1.3	0.74
162837/2667534	68	-1.9	0.41	CEM	62	1.1	0.47	1	3.1	1.3e+02	8.8	1.2
162837/3805090	36	1.3	-0.057	CEM	44	-2	0.11	1	3	79	0.62	2.1
162937/5236760	30	2.9	0.57	CEM	37	0.86	-0.71	1	2.1	73	4.5	4.2
162986/1567868	29	-0.38	-0.66	CEM	36	-2.5	-0.94	1	2.1	57	9.1	0.74
162986/2571751	41	-2	-0.89	CEM	38	1.1	0.18	1	3.1	90	3.6	0.83
163012/1193692	46	1.8	0.5	CEM	27	-1.4	-0.66	1	3.1	82	9.2	5.2
163024/33079	36	-0.039	0.77	CEM	47	-3	0.55	1	2.9	82	11	0.0064
163024/334959	28	2.5	0.75	CEM	53	-0.091	-0.55	1	2.5	90	13	3.8
163064/1565248	37	-0.89	-0.85	CEM	53	2.3	0.6	1	3.1	1.1e+02	1.4	4.4
163064/7705584	26	-1.3	0.94	CEM	32	-3	-0.068	1	1.7	52	34	0.77
163394/997182	39	-0.23	-0.98	CEM	39	3	-0.18	1	3.1	86	2.8	1.2
163431/1462399	32	-0.54	-0.4	CEM	28	0.03	-0.32	1	0.57	17	50	2.9
165412/8429992	36	-1.4	0.35	CEM	48	1.4	-0.2	1	2.8	86	7.5	2.8
165412/9099249	34	-2.7	0.51	CEM	30	0.9	-0.3	1	2.7	68	6.2	5.3
165435/1442336	49	-0.47	0.52	CEM	44	2.8	0.71	1	3	92	3.9	3.5
165435/2295612	27	-0.7	0.61	CEM	27	3	1	1	2.5	53	9.1	3
164844/890472	47	-2.1	-0.94	CEM	35	1.1	-1	1	3	81	11	1.1
164844/6642760	27	-0.66	-0.069	CEM	60	-2.9	0.88	1	2.3	83	12	1.1
				CEM	36	0.54	0.98	1	1.2	49		
165271/1518816	34	-2.6	-0.079	CEM	40	0.57	0.74	1	3.1	81	5.1	4.2
165271/6720684	39	1.7	-0.86	CEM	36	-1.4	0.29	0	3.1	89	4.1	2
165313/1216784	32	1.3	-0.058	CEM	49	1.8	0.36	0	0.51	26	15	5.5
165313/3259180	46	2.5	0.2	CEM	45	-0.47	0.3	1	2.9	90	2.3	5.1
165388/3815600	53	0.87	1	CEM	50	-2.2	0.58	1	3	1e+02	0.52	0.7
165412/1019218	39	-0.35	0.83	CEM	58	0.86	-0.59	1	1.2	92	18	3.3
165836/37863	38	0.95	0.81	CEM	59	-2.3	0.85	1	3.1	95	13	0.027
165871/281298	28	2.9	0.082	CEM	30	-0.38	-0.13	1	3	59	5.7	0.95
165873/5395948	43	-0.41	-1	CEM	34	3	0.18	1	2.9	92	9.5	0.39
165873/6389470	27	2.6	0.74	CEM	30	-0.36	-0.5	1	2.9	66	9.3	6.2
165902/3923959	37	-2	-0.086	CEM	47	1.2	0.81	1	3	92	5.3	0.39
165906/4665906	69	-0.22	0.079	CEM	50	2.9	-0.36	1	3.1	1.2e+02	6.3	2.6
165906/6178779	29	-2	0.98	CEM	26	1.2	0.93	1	3.1	55	4.7	0.5
165906/6899039	39	0.58	0.75	CEM	56	-2.8	0.56	1	2.9	94	11	6.2
165944/2371443	47	1.6	0.19	CEM	36	-1.5	-0.7	1	3.1	90	10	4.7
166037/154184	28	-2.4	-0.2	CEM	35	0.66	-0.46	1	3.1	63	2.7	1.8
166038/1616859	32	-1.4	-0.24	CEM	40	1.8	-0.82	1	3.1	74	16	0.43
166038/6509526	31	2.3	0.36	CEM	30	-1.9	0.96	1	2.1	58	4.2	2.9
				CEM	22	-0.13	-0.15	1	2.4	51		
166073/950323	46	2.6	0.59	CEM	40	-0.63	-0.42	1	3.1	96	11	5.7
166251/203578	25	-2.9	-0.28	CEM	30	1.2	-0.72	1	2.2	51	8.5	4.9
166251/1524593	43	2.8	0.53	CEM	41	-0.33	-0.17	1	3.1	90	3.4	3.2
166325/255125	25	0.55	0.73	CEM	85	-2.3	1	1	2.9	92	30	0.53
166328/625466	47	2.1	1	CEM	41	-0.97	0.61	1	3.1	89	14	5.3
166472/63997	29	0.33	0.22	CEM	55	-2.9	-0.6	1	3	86	19	6.2
166479/1662364	50	-0.65	0.18	CEM	53	2.4	-0.51	1	3.1	1.1e+02	13	5.3
166479/8916078	43	-2.7	-0.73	CEM	53	0.87	-0.67	1	2.7	93	5.2	5.1
166525/442568	41	-1.7	0.56	CEM	53	1.4	0.51	1	3.1	93	2.4	0.36
166529/3814797	25	-0.15	0.45	CEM	35	2.4	0.28	1	2.6	57	13	4.6
166567/4896270	37	-0.29	0.41	CEM	36	2.8	-0.93	1	3	88	7.4	5.7

Continued on next page

Table 29 – continued from previous page

150823/36469	37	-2.2	0.61	CEM	30	0.9	0.96	1	3.1	67	3.2	5.1
166653/2246548	47	-1.3	-0.9	CEM	35	0.98	0.36	1	2.3	92	1.1	5.7
166657/328363	42	2.2	-0.84	CEM	50	-0.82	-0.91	1	3	91	0.8	4.9
166715/662481	39	-1.4	0.17	CEM	45	1.9	0.39	1	3	84	9	5.5
166771/1079504	31	-0.7	-0.053	CEM	25	2.7	0.54	1	2.9	58	1.6	2.8
166783/1159285	28	-2.5	-0.17	CEM	31	0.3	0.9	1	2.8	68	4.2	5.7
166805/3046265	48	2.8	0.98	CEM	56	-0.23	-0.18	0	3.1	1.2e+02	2.3	4.7
166927/827910	44	-2.5	-0.43	CEM	45	0.84	-0.2	1	3	89	6.3	5.5
166927/5409041	43	-3	0.69	CEM	48	0.57	0.42	1	2.7	90	13	5.2
167022/15	36	-0.92	0.14	CEM	35	2.5	-0.34	1	2.9	72	5.9	0.6
167022/403494	33	-1.7	-0.31	CEM	36	1.3	-0.91	1	2.9	72	8.9	0.7
167025/379798	27	0.75	0.95	CEM	30	-2.3	-0.34	1	3.1	69	4.1	1.2
167053/2182242	42	-0.81	0.22	CEM	48	3.1	-0.31	1	2.4	87	9.8	0.93
167053/9626664	31	0.5	-0.39	CEM	42	-2.7	0.18	1	3.1	74	15	0.14
167053/9941444	85	0.87	-0.36	CEM	1e+02	-2.2	-0.1	1	3.1	1.9e+02	8.2	1.3
167138/1352871	34	1.8	0.18	CEM	39	-1.5	0.93	1	3	79	1.9	4.9
167139/248903	29	0.16	0.5	CEM	51	-2.6	-0.87	1	2.8	95	23	0.68
167259/1405391	46	-2.7	-0.31	CEM	42	0.3	-0.049	1	3	88	8	1.3
167506/2764767	41	-1.4	0.085	CEM	50	1.9	0.95	1	3	98	4.9	5.3
167266/73079	38	-1	0.63	CEM	29	2.4	-0.44	1	2.9	76	6.6	5.1
167299/670904	26	2.3	-0.77	CEM	26	1.9	-0.43	1	0.37	13	40	5.2
144942/3176804	45	0.13	0.26	CEM	41	2.8	0.82	1	2.7	87	6.3	4.2
151116/446939	38	1.6	-0.8	CEM	39	-1.2	-0.35	1	2.8	78	4.6	3.5
167506/212585	27	0.35	0.58	CEM	68	-2.7	0.32	1	3.1	86	14	6.2
167506/5483781	35	-3	-0.2	CEM	40	0.19	0.21	1	3.1	76	2.9	3.9
167551/4201514	31	-2.9	0.61	CEM	33	0.96	-0.37	1	2.4	68	7.4	5.8
167565/437210	34	-2.4	-0.76	CEM	33	0.62	-0.17	1	3	69	0.65	3.5
151238/162602	31	2.7	-0.54	CEM	30	-0.14	-0.82	1	2.9	61	5.8	4.5
151434/1325990	60	-2.7	-0.75	CEM	39	0.21	-0.86	1	2.9	96	9.5	1.3
151434/1968552	30	-0.96	-0.84	CEM	32	2.1	-1	1	3.1	62	6.6	5.2
167623/4691216	27	1.9	0.7	CEM	30	1.7	0.21	1	0.21	14	19	4.8
				CEM	21	-1.5	-0.72	1	2.9	60		
167623/6299171	51	1.2	-0.86	CEM	54	-1.8	-0.4	1	3	1.1e+02	11	3.4
167629/663851	34	-2.8	0.63	CEM	65	-0.82	-0.22	1	2	89	6.1	2.6
167715/48131	40	2.3	0.29	CEM	42	-0.96	-0.68	1	3	91	6.8	1.8
167715/1327864	43	-2.3	-0.75	CEM	40	0.85	-1	1	3.1	83	6.6	0.56
167715/2018922	52	-0.62	0.98	CEM	62	2.5	0.9	1	3.1	1.1e+02	1.5	5.7
167824/1722825	28	2.7	0.39	CEM	30	-0.5	0.35	1	3.1	58	1.9	5.6
167824/2643942	42	-3.1	-0.68	CEM	37	-0.94	0.72	1	2.1	92	12	0.12
167849/2063706	50	3.1	0.89	CEM	41	1.3	-0.14	1	1.8	85	44	5.7
167866/443088	69	-1.3	-0.29	CEM	98	-1.3	0.54	1	0.026	70	4.8	0.81
151476/246871	43	2.3	-0.18	CEM	47	-0.94	0.59	1	3.1	96	7.3	4.7
151476/1085329	30	1.7	-0.61	CEM	38	-1.4	-0.87	1	3.1	68	6.7	1.8
167955/807879	27	-0.043	0.23	CEM	29	3.1	0.42	1	3.1	56	7.8	0.49
167977/1654370	29	1.1	-0.69	CEM	29	-2	-0.39	1	3.1	59	2.6	1.7
167977/5204069	36	-0.7	-0.53	CEM	39	2.4	0.46	1	3.1	84	8	5.3
167997/2967480	68	3.1	1	CEM	44	-0.46	0.83	1	2.7	1.1e+02	16	6.1
151477/174189	43	-1.2	-0.27	CEM	42	2	-0.64	1	3.1	86	3.5	4.7
168125/134814	50	-2.5	-0.43	CEM	35	0.7	-0.34	1	3	84	14	0.22
168563/279980	30	2.7	-0.55	CEM	43	-0.91	-0.52	1	2.7	70	10	1.4

Continued on next page

Table 29 – continued from previous page

168599/1466473	40	-2.6	0.23	CEM	49	0.63	0.1	1	3.1	89	7.4	0.72
168599/1871793	36	-2	0.67	CEM	29	0.85	0.63	1	2.8	64	3.3	1.1
168599/3868597	33	0.89	0.72	CEM	54	-1.7	-0.66	1	2.6	1e+02	25	2.5
168766/292613	34	0.66	0.98	CEM	37	-2.4	-0.3	1	3.1	85	3.7	0.43
168769/205130	43	2.8	-0.34	CEM	50	-0.68	-0.74	1	2.8	93	14	2.2
168775/283381	34	0.65	0.69	CEM	30	-2.2	-0.91	1	2.8	83	7.3	1.4
168820/3064053	30	0.91	-0.17	CEM	43	-2.2	0.9	1	3.1	82	7.9	1.1
168889/8234247	79	-2.7	-0.35	CEM	74	0.46	0.16	1	3.1	1.6e+02	6.2	0.41
145035/1185532	42	-0.032	0.97	CEM	27	2.9	0.45	1	3	70	20	3.6
143847/2782165	48	0.03	0.12	CEM	43	-3.1	0.14	1	3.1	91	4.2	3.2
143981/3060545	34	1.7	0.43	CEM	33	-2	-0.053	1	2.6	67	3	2.4
144424/2437736	35	-0.85	-0.96	CEM	38	2.2	0.54	1	3	96	12	5.2
151688/69756	58	-2.5	0.19	CEM	51	0.74	0.66	1	3.1	1.1e+02	8	0.27
151844/1409167	41	2.8	0.62	CEM	42	-0.5	-0.13	1	3	89	5.2	1.7
160988/2882911	84	-0.97	-0.47	CEM	69	2.1	0.11	1	3.1	1.6e+02	7.2	2.8
164625/1792236	38	0.91	-0.64	CEM	27	1.4	0.76	1	0.49	51	20	3.9
163474/688137	27	-2.4	0.78	CEM	60	0.67	0.76	1	3	81	13	3.7
163526/14750	25	-2.1	-0.46	CEM	31	1.3	-0.54	0	2.9	56	27	5.4
164107/164310	26	-2.3	-0.59	CEM	31	0.65	-0.16	1	3	58	6.8	2.4
164126/98062	34	3.1	0.64	CEM	39	0.028	0.078	1	3.1	76	9.2	6.2
164259/131630	33	1.7	-0.45	CEM	41	-1.9	-0.33	1	2.7	72	6.8	5.8
164304/459451	30	2.4	0.25	CEM	34	-1.4	0.79	1	2.5	62	9	0.85
164354/2156076	40	-0.71	0.39	CEM	46	2.3	0.63	1	3	85	4.6	0.22

Table 29: List Of Electron-Photon Events

	γ			ℓ					$\ell\gamma$		$\not\!\!E_T$	
run/event	pt	phi	eta	type	pt	phi	eta	trg	dphi	InvM	$\not\!\!E_T$	phi
153074/1339595	26	-0.33	-0.18	CEM	40	-1.3	-0.99	1	1	40	27	0.47
153662/723772	25	0.94	-0.9	CEM	32	1.2	0.59	0	0.21	45	54	4.1
156083/1091219	35	2.1	-0.19	CEM	33	1.1	0.37	1	1.1	40	60	4.7
162836/996381	62	2.8	0.41	CEM	59	-0.72	0.22	1	2.8	1.2e+02	25	6.1
163064/7705584	26	-1.3	0.94	CEM	32	-3	-0.068	1	1.7	52	34	0.77
163431/1462399	32	-0.54	-0.4	CEM	28	0.03	-0.32	1	0.57	17	50	2.9
166325/255125	25	0.55	0.73	CEM	85	-2.3	1	1	2.9	92	30	0.53
167299/670904	26	2.3	-0.77	CEM	26	1.9	-0.43	1	0.37	13	40	5.2
167849/2063706	50	3.1	0.89	CEM	41	1.3	-0.14	1	1.8	85	44	5.7
163526/14750	25	-2.1	-0.46	CEM	31	1.3	-0.54	0	2.9	56	27	5.4

Table 30: List Of Electron-Photon-Met Events

8.2.2 Muon-Photon Events

	γ			ℓ					$\ell\gamma$		$\not\!\!E_T$	
run/event	pt	phi	eta	type	pt	phi	eta	trg	dphi	InvM	$\not\!\!E_T$	phi
Continued on next page												

Table 32 – continued from previous page

165439/568710	44	1.1	0.17	CMUP	45	-2.2	0.34	1	3.1	89	4.4	-1.8
149677/68423	28	-0.15	0.87	CMUP	41	-2.1	-0.28	1	1.9	71	44	2
166653/3270001	30	-0.029	0.43	CMUP	27	0.63	0.51	1	0.66	18	48	-2.8
166927/295457	27	1.8	0.61	CMUP	41	-1.2	-0.45	1	3	74	6.4	2.7
167023/7639345	37	1.8	-0.58	CMUP	29	-1.9	-0.27	1	2.6	65	11	-0.24
167137/57423	35	2.4	0.11	CMUP	27	-0.9	-0.49	1	3	63	4.2	2.2
167849/3096656	46	-0.75	-0.9	CMUP	28	2.8	0.19	1	2.7	81	0.25	-2.9
167955/33039	28	-2.7	0.58	CMUP	56	-0.036	0.31	1	2.6	78	6.5	0.24
				CMIO	34	2.6	-10	1	1	30		
153739/175671	28	-1.4	0.78	CMUP	42	-1.3	0.26	1	0.15	17	33	-0.52
151135/326271	31	1.7	-0.9	CMUP	30	0.7	-0.39	1	0.99	33	2.6	0.11
				CMIO	29	-2.1	-10	1	2.5	58		
151843/1584392	25	-1.6	0.1	CMUP	41	3.1	-0.21	1	1.6	48	49	0.74
152267/173349	32	-2.7	-0.27	CMUP	34	-0.36	0.094	1	2.3	61	17	1.2
152507/1700045	35	0.99	-0.96	CMX	65	-3	-0.73	1	2.3	88	7.6	-0.93
				CMUP	27	0.059	-0.47	1	0.93	31		
143281/920862	48	-2.1	-0.39	CMX	35	0.25	-0.64	1	2.4	76	3.8	2.5
				CMUP	32	1.5	-0.047	1	2.6	77		
155895/6336800	59	2.3	-0.29	CMUP	53	-0.056	0.24	1	2.4	1.1e+02	35	-1.7
156089/1783191	27	-2.8	-0.84	CMX	39	0.5	-0.73	1	3	65	6.6	-0.19
				CMUP	26	-2.7	-0.38	1	0.044	13		
160410/1899784	38	-2.4	-1	CMUP	40	0.58	0.13	1	3	90	3.9	-2.3
162686/2327952	58	0.1	-0.23	CMUP	82	0.86	0.33	1	0.75	64	55	-2.6
162837/1710782	38	-1.1	0.38	CMUP	28	-3.1	0.55	1	1.9	54	20	1.7
160823/7078294	30	-0.22	0.26	CMUP	43	2.9	-0.2	1	3.1	73	14	0.17
161330/9896	36	-1.7	1	CMUP	32	0.32	0.24	1	2	63	15	2.1
161330/3293805	26	-0.22	0.32	CMUP	42	2.6	0.11	1	2.8	64	5.9	3
				CMIO	22	-0.7	-10	1	0.48	13		
162100/303455	39	2.1	-0.48	CMUP	55	-0.84	0.35	1	3	98	14	2.4
162238/185410	29	-2.3	-0.24	CMUP	61	-0.12	-0.26	0	2.1	75	6.3	2.9
				CMP	38	1.8	0	0	2.2	66		
162423/3147780	46	2.9	0.49	CMUP	51	-0.33	0.31	1	3.1	97	6	1.5
165201/298019	26	2.5	0.55	CMUP	36	-0.48	-0.35	1	3	67	10	-1.7
165388/5194587	28	-1.3	0.99	CMUP	43	1.7	0.35	1	3.1	73	11	-1.7
165388/5538230	34	2	1	CMUP	41	-1.2	0.14	1	3.1	81	3.7	1.6

Table 32: List Of Muon-Photon Events

	γ			ℓ					$\ell\gamma$		$\not{E}_{\mathrm{T}}$	
run/event	pt	phi	eta	type	pt	phi	eta	trg	dphi	InvM	$\not{E}_{\mathrm{T}}$	phi
154518/1101736	83	-1.5	-0.14	CEM	48	1.4	-0.72	1	2.9	1.3e+02	1.9	6.3
				EPLUG	46	1.9	-2.4	1	2.8	2.2e+02		
162396/1323030	27	0.55	-0.99	CEM	42	-2.8	-0.95	1	2.9	66	5.4	0.75
				CEM	21	0.15	-0.39	1	0.4	16		
149387/1099516	30	3.1	-0.36	CEM	57	-0.42	-0.38	1	2.7	80	10	5
				CEM	31	2.4	0.45	1	0.7	33		
160346/1528176	46	-0.82	-0.87	CEM	50	-3.1	-1	1	2.3	88	16	1.4
				CEM	25	0.81	-0.94	1	1.6	49		
164844/6642760	27	-0.66	-0.069	CEM	60	-2.9	0.88	1	2.3	83	12	1.1
				CEM	36	0.54	0.98	1	1.2	49		
166038/6509526	31	2.3	0.36	CEM	30	-1.9	0.96	1	2.1	58	4.2	2.9
				CEM	22	-0.13	-0.15	1	2.4	51		
167623/4691216	27	1.9	0.7	CEM	30	1.7	0.21	1	0.21	14	19	4.8
				CEM	21	-1.5	-0.72	1	2.9	60		

Table 31: List Of Multi-Electron, Multi-Photon Events

	γ			ℓ					$\ell\gamma$		$\not{E}_{\mathrm{T}}$	
run/event	pt	phi	eta	type	pt	phi	eta	trg	dphi	InvM	$\not{E}_{\mathrm{T}}$	phi
149677/68423	28	-0.15	0.87	CMUP	41	-2.1	-0.28	1	1.9	71	44	2
166653/3270001	30	-0.029	0.43	CMUP	27	0.63	0.51	1	0.66	18	48	-2.8
153739/175671	28	-1.4	0.78	CMUP	42	-1.3	0.26	1	0.15	17	33	-0.52
151843/1584392	25	-1.6	0.1	CMUP	41	3.1	-0.21	1	1.6	48	49	0.74
155895/6336800	59	2.3	-0.29	CMUP	53	-0.056	0.24	1	2.4	1.1e+02	35	-1.7
162686/2327952	58	0.1	-0.23	CMUP	82	0.86	0.33	1	0.75	64	55	-2.6

Table 33: List Of Muon-Photon-Met Events

	γ			ℓ					$\ell\gamma$		$\not{E}_T$	
run/event	pt	phi	eta	type	pt	phi	eta	trg	dphi	InvM	$\not{E}_T$	phi
167955/33039	28	-2.7	0.58	CMUP	56	-0.036	0.31	1	2.6	78	6.5	0.24
				CMIO	34	2.6	-10	1	1	30		
151135/326271	31	1.7	-0.9	CMUP	30	0.7	-0.39	1	0.99	33	2.6	0.11
				CMIO	29	-2.1	-10	1	2.5	58		
152507/1700045	35	0.99	-0.96	CMX	65	-3	-0.73	1	2.3	88	7.6	-0.93
				CMUP	27	0.059	-0.47	1	0.93	31		
143281/920862	48	-2.1	-0.39	CMX	35	0.25	-0.64	1	2.4	76	3.8	2.5
				CMUP	32	1.5	-0.047	1	2.6	77		
156089/1783191	27	-2.8	-0.84	CMX	39	0.5	-0.73	1	3	65	6.6	-0.19
				CMUP	26	-2.7	-0.38	1	0.044	13		
161330/3293805	26	-0.22	0.32	CMUP	42	2.6	0.11	1	2.8	64	5.9	3
				CMIO	22	-0.7	-10	1	0.48	13		
162238/185410	29	-2.3	-0.24	CMUP	61	-0.12	-0.26	0	2.1	75	6.3	2.9
				CMP	38	1.8	0	0	2.2	66		

Table 34: List Of Multi-Muon, Multi-Photon Events

	γ			ℓ					$\ell\gamma$		$\not{E}_T$	
run/event	pt	phi	eta	type	pt	phi	eta	trg	dphi	InvM	$\not{E}_T$	phi
167137/57423	35	2.4	0.11	EPLUG	19	-0.73	-1.5	0	3.1	69	4.2	2.2
				CMUP	27	-0.9	-0.49	1	3	63		

Table 35: List Of Electron+Muon+Photon Events

References

[1] S. L. Glashow. *Nucl. Phys.*, 22, 1961.

[2] S. Weinberg. *Phys. Rev. Lett.*, 19, 1967.

[3] A. Salam. *Proc. 8th Nobel Symposium, Stockholm*, 1979.

[4] S.Ambrosanio, G.L.Kane, G.D.Kribs, S.P.Martin, and S.Mrenna. hep-ph/9607414, 1996.

[5] S. P. Martin. *A Supersymmetry Primer, in Perspectives on Supersymmetry,* G. Kane, editor. Singapore: World Scientific, 1998.

[6] K.Sridhar B.C.Allanach, S.Lola. hep-ph/0111014, 2001.

[7] S.M. Berman, J.D. Bjorken, and J.B. Kogut. *Phys. Rev. D*, 4, 1971.

[8] J. D. Lykken. Physics of Extra Dimensions. Prepared for Theoretical Advanced Study Institute in Elementary Particle Physics (TASI 2000): Flavor Physics for the Millennium, Boulder, Colorado, 4-30 Jun 2000.

[9] Al Goshaw, Beate Heinemann, Helen Hayward, Michael Kirby, and Naho Tanimoto. Measurement of W+gamma and Z+gamma Production in $\bar{p}p$ Collisions at $\sqrt{s} = 1.96$ gev (to be submitted to PRL). CDF Note 7141, CDF, 2004.

[10] T. Affolder et al. Searches for new physics in events with a photon and b-quark jet at CDF. *hep-ex/0106012,* Phys. Rev. D65:052006, 2002.

[11] T. Affolder et al. Search for new physics in photon-lepton events in proton-antiproton collisions at $\sqrt{s} =$ 1.8 tev. *hep-ex/0110015,* Phys. Rev. D66:012004, 2001.

[12] F. Abe et al. The CDF detector: An overview. *Nucl. Instrum. Meth. Phy. Res., Sect. A*, 271:387–403, 1988.

[13] F. Abe et al. The CDF 2 detector technical design report. CDF Note FERMILAB-Pub-96/390-E, CDF, 1996.

[14] CDF Collaboration. The CDF 2 detector technical design report. CDF Webpage http://www-cdf.fnal.gov/upgrades/upgrades.html, CDF, 1996.

[15] E.J. Thomson. Description of data samples for top and electroweak groups for winter 2003. CDF Note 6265, CDF, 2003.

[16] P. Onyisi and the UC CDF Physics Group. The ucntuple is described on the web page:—. http://hep.uchicago.edu/cdf/flatntuple, 2004.

[17] See http://www-cdf.fnal.gov/ konigsb/lum_official_page.html.

[18] Jian Kang Ken Bloom, Eric James et al. Updated Measurements of $\sigma(\bar{p}p \to \mu\nu)$,$\sigma(\bar{p}p \to Z \to \mu\mu)$, and R using CDF Run II Data. CDF Note 6302, CDF, 2003.

[19] V. Martin. High pt efficiencies, recommended cuts and efficiencies for release 5.3.1. CDF Note 7031, CDF, 2004.

[20] Lauren Beitler. Talk given to the W+Jets Meeting, Oct. 10, 2003.

[21] Anyes Taffard. Run II cosmic ray tagger. CDF Note 6100, CDF, 2003.

[22] Anyes Taffard. Run II cosmic ray tagger perfomances. CDF Note 6255, CDF, 2003.

[23] Giulia Manca Young-Kee Kim. Z^0 to electrons cross section measurement with Run II data. CDF Note 6281, CDF, 2003.

[24] Andy Hocker Mircea Coca, Eva Halkiadakis et al. Wenu cross section analysis with run II data. CDF Note 6300, CDF, 2003.

[25] P.J. Wilson. Calorimeter isolation and lateral shower leakage for photons and electrons. CDF Note 4170, CDF, 1997.

[26] T. Stelzer and W. F. Long. Madgraph. *Comput.Phys.Commun.*, 357(81), 1994.

[27] F. Maltoni and T. Stelzer. Madgraph. *ILL-(TH)-02-9*, 2002.

[28] M. Dubinin A. Pukhov, E. Boos et al. Comphep: A package for evaluation of Feynman diagrams and integration over multiparticle phase space. By A. Pukhov, E. Boos, M. Dubinin, V. Edneral, V. Ilyin, D. Kovalenko, A. Kryukov, V. Savrin (Moscow State U.), S. Shichanin (Serpukhov, IHEP), A. Semenov (Dubna, JINR). INP-MSU-98-41-542, Aug 1999. 126pp. User's manual for version 33. e-Print Archive: hep-ph/9908288; E.E. Boos, M.N. Dubinin, V.A. Ilyin, A.E. Pukhov, and V.I. Savrin, INP MSU 94-36/358 and SNUTP-94-116, hep-ph/9503280; P. Baikov *et al.*, in Proc. of the Xth Int. Workshop on High Energy Physics and Quantum Field Theory, QFTHEP-95, ed. by B. Levtchenko and V. Savrin, (Moscow, 1995), p. 101.

[29] Uli Baur and Stephen Mrenna. Monte carlo event generator program. http://www.hep.anl.gov/theory/mrenna/sources/uli.uu.

[30] A.S. Thompson S. Tsuno. A CDF-interface module for Les Houches Accords. CDF Note 6333, CDF, 2003.

[31] Henry Frisch and Chadd Smith. Predicted cross sections for w+photon and z+photon production. CDF Note 6057, CDF.

[32] Beate Heinemann Doug Benjamin, Al Goshaw et al. Theoretical predictions of w+gamma and z+gamma production in Run II. CDF Note 6619, CDF, 2004.

[33] Dan Amidei, Ken Bloom, Mircea Coca, Eva Halkiadakis, Eric James, et al. Measurements of $\sigma * B(W \to e\nu)$, $\sigma * B(Z \to ee)$ and the ratio R using CDF Run II Data. Cdf note, CDF, 2004.

[34] Beate Heinemann Helen Hayward. Update on the measurement of the probability of a jet faking an isolated photon. CDF Note 6838, CDF, 2004.

[35] Beate Heinemann Helen Hayward. The probability of a jet faking an isolated photon. CDF Note 6363, CDF, 2003.

[36] We have added one category: Events with exactly one lepton and exactly one photon, but not back-to-back.